

Dynamically massive linear covariant gauges: Setup and first resultsGiorgio Comitini^{1,2,3,*} Tim De Meerleer^{3,†} David Dudal^{3,4,‡} and Silvio Paolo Sorella^{5,§}¹*Department of Physics and Astronomy, University of Catania, Via Santa Sofia 64, I-95123 Catania, Italy*²*INFN Sezione di Catania, Via Santa Sofia 64, I-95123 Catania, Italy*³*KU Leuven Campus Kulak Kortrijk, Department of Physics,
Etienne Sabbelaan 53 bus 7657, 8500 Kortrijk, Belgium*⁴*Department of Physics and Astronomy, Ghent University, Krijgslaan 281-S9, 9000 Gent, Belgium*⁵*Departamento de Física Teórica, Instituto de Física, UERJ-Universidade do Estado do Rio de Janeiro,
Rua São Francisco Xavier 524, 20550-013 Maracanã, Rio de Janeiro, Brazil*

(Received 11 December 2023; accepted 5 January 2024; published 30 January 2024)

We discuss the possibility to obtain a massive Landau gauge, based on the local composite operator effective action framework combined with the Zimmermann reduction of couplings prescription. As a way to deal with the gauge ambiguity, we check that the ghost propagator remains positive, a necessary condition for gluon field configurations beyond the Gribov region to be negligible. We pay attention to the Becchi-Rouet-Stora-Tyutin invariance of the construction, allowing for a future generalization to a class of massive linear covariant gauges. As a litmus test, we compare our predictions to the lattice data for the two-point functions in Landau gauge introducing the “dynamically infrared-safe” renormalization scheme, including the renormalization group optimization of both the gap equation and the two-point functions. We also discuss the relation to and differences with the Curci-Ferrari model, the usefulness of which in providing an effective perturbative description of nonperturbative Yang-Mills theories became clear during recent years.

DOI: [10.1103/PhysRevD.109.014037](https://doi.org/10.1103/PhysRevD.109.014037)**I. INTRODUCTION**

Recently, the Curci-Ferrari (CF) model [1,2] has witnessed a revived interest in works like [3–11] thanks to its capability to describe rather well the n -point functions of gauge theories in the Landau gauge, next to allowing a perturbative sneak peek into the phase diagram [12–14]. As of now, however, the success in matching the model to lattice data relies on the fitting of both the gauge coupling g and the Curci-Ferrari mass m [4,5,8].

A possible route toward a first-principle derivation of the model, including a determination of m from the sole knowledge of g at a given scale, was formulated in [15] based on a weighing over the Gribov copies. It was implemented successfully in a class of nonlinear gauges that contains the Landau gauge as a limiting case [16]. Unfortunately, the dynamical mass generation mechanism identified in this reference fails precisely in this limit.

A more recent attempt was done in [17], directly in the Landau gauge. It was found that the system exhibits two phases, one of which corresponds to a massive implementation of the Landau gauge bearing some resemblance with the Curci-Ferrari model, with however gapped ghost degrees of freedom. As discussed in [17], the presence of massive ghosts is not incompatible with the lattice results, for the latter are not a direct measurement of the ghost propagator but rather the averaging of the Faddeev-Popov operator $-\partial_\mu D_\mu$ which remains massless in both of the above mentioned phases. A more serious difficulty is, however, that the gluon mass identified in [17] appears as a mere gauge-fixing parameter whose value is not determined in terms of g . Although it remains yet to be seen how much the correlators computed within this approach are sensitive to this gauge-fixing parameter, this could potentially compromise the comparison to lattice data.

On the other hand, it has been known for some time that dimension-two condensates such as $\langle A_\mu^a A_\mu^a \rangle$ can be dynamically generated in the Landau gauge via the local composite operator (LCO) formalism [18] and the minimization of the vacuum energy. A natural question that emerges is then what connection do these condensates bear with the Curci-Ferrari model (or similar approaches), and to which extent do they allow one to reproduce the Landau gauge correlators evaluated on the lattice. The current note aims at investigating these questions. Since our goal is to eventually extend the approach to covariant gauges, we will pay

*giorgio.comitini@dfa.unict.it

†timdemeerleer07@gmail.com

‡david.dudal@kuleuven.be

§sorella@uerj.br

Published by the American Physical Society under the terms of the [Creative Commons Attribution 4.0 International license](https://creativecommons.org/licenses/by/4.0/). Further distribution of this work must maintain attribution to the author(s) and the published article's title, journal citation, and DOI. Funded by SCOAP³.

particular attention to the Becchi-Rouet-Stora-Tyutin (BRST) invariance of the construction.

Two-dimensional condensates are of course not free of ambiguities due to their composite nature that requires extra renormalization. However, since the correlators of the primordial fields do not depend on this additional subtractions, at least not at an exact level, it is possible to exploit the reduction of coupling technique [19,20] in order to fix this arbitrariness in some way, as we recall below. In fact, one could envisage using similar ideas to fix the arbitrariness in the choice of the gluon mass in the approach of [17], at least for the evaluation of physical observables.

II. THE BRST-INVARIANT CONDENSATE

A. BRST-invariant gauge field

Our starting point is the Euclidean Yang-Mills action in $d = 4 - \varepsilon$ dimensions supplemented with a linear covariant gauge fixing:

$$S_{\text{YM}}^{(1)} = \int d^d x \left(\frac{1}{4} F_{\mu\nu}^a F_{\mu\nu}^a + \frac{\alpha}{2} b^2 + i b^a \partial_\mu A_\mu^a + \bar{c}^a \partial_\mu D_\mu^{ab} c^b \right) \quad (1)$$

with $F_\mu^a = \partial_\mu A_\nu^a - \partial_\nu A_\mu^a + g f_{bc}^a A_\mu^b A_\nu^c$ the non-Abelian field-strength tensor and $D_\mu^{ab} = \delta^{ab} \partial_\mu + g f^{acb} A_\mu^c$ the covariant derivative in the adjoint representation. Since our choice is to preserve BRST invariance at each step, we should only consider BRST-invariant gluon mass operators, constructed out of a BRST-invariant version of the gauge field. To this purpose, we insert into the corresponding path integral a unity $1 = \mathcal{N} \int \mathcal{D}\xi \mathcal{D}\tau \mathcal{D}\bar{\eta} \mathcal{D}\eta e^{-S_1} \det(\Lambda(\xi))$, with

$$S_1 = \int d^d x (\tau^a \partial_\mu A_\mu^{h,a} + \bar{\eta}^a \partial_\mu D_\mu^{ab} (A^h) \eta^b) \quad (2)$$

and

$$\Lambda_{ab}(\xi) = \frac{2i}{g} \text{Tr} \left\{ t_a \frac{\partial h^\dagger}{\partial \xi^b} h \right\}, \quad (3)$$

the appropriate normalization being collected in \mathcal{N} . Here, we introduced the local but nonpolynomial composite field

$$A_\mu^h \equiv A_\mu^{h,a} t^a = h^\dagger A_\mu h + \frac{i}{g} h^\dagger \partial_\mu h, \quad (4)$$

with

$$h = e^{ig\xi} = e^{ig\xi^a t^a}, \quad (5)$$

where the t^a denote the generators of the $su(N)$ algebra and the ξ^a are akin to Stueckelberg fields. The fields $\bar{\eta}^a$ and η^a are additional (anticommuting) ghosts that, together with the ξ -dependent determinant $\det(\Lambda(\xi))$, account for the

Jacobian arising from the change of variables $\xi \rightarrow A^h$, which is itself needed in order to treat the functional distribution $\delta(\partial_\mu A_\mu^h)$ that appears after integration over τ . As we will show in Appendix A, so long as the theory is defined in dimensional regularization, the determinant gives no contribution to the partition function at any fixed order in perturbation theory. For this reason, in what follows we will drop $\det(\Lambda(\xi))$ and write the unity in the form $1 = \mathcal{N} \int \mathcal{D}\xi \mathcal{D}\tau \mathcal{D}\bar{\eta} \mathcal{D}\eta e^{-S_1}$.

We stress that, when writing equations such as (1) or (2), we are disregarding the presence of Gribov copies. The justification is twofold. First, in this work, we restrict to perturbation theory for the evaluation of both the correlation functions and the vacuum energy. Second, we will soon check that the dynamically generated condensate is such that the ghost propagator remains positive, a necessary condition for the functional integral to be dominated by configurations within the first Gribov region.

The action (2) is here used as a way to treat, within a local setup, a BRST-invariant quantity A_μ^h that becomes nonlocal on shell. The nonlocal on-shell nature of A_μ^h becomes explicit after one solves the condition $\partial_\mu A_\mu^h = 0$ iteratively for ξ using

$$(A^h)_\mu^a = A_\mu^a - \partial_\mu \xi^a - g f^{abc} A_\mu^b \xi^c - \frac{g}{2} f^{abc} \xi^b \partial_\mu \xi^c + \dots \quad (6)$$

Indeed, this leads to the infinite series of terms:

$$\xi = \frac{\partial A}{\partial^2} + i \frac{g}{\partial^2} \left[\partial A, \frac{\partial A}{\partial^2} \right] + i \frac{g}{\partial^2} \left[A_\mu, \partial_\mu \frac{\partial A}{\partial^2} \right] + \frac{i}{2} \frac{g}{\partial^2} \left[\frac{\partial A}{\partial^2}, \partial A \right] + \dots, \quad (7)$$

which eventually gives the transverse on-shell expression

$$A_\mu^h = \left(\delta_{\mu\nu} - \frac{\partial_\mu \partial_\nu}{\partial^2} \right) \phi_\nu, \quad (8)$$

with

$$\phi_\nu = A_\nu - ig \left[\frac{\partial A}{\partial^2}, A_\nu \right] + \frac{ig}{2} \left[\frac{\partial A}{\partial^2}, \partial_\nu \frac{\partial A}{\partial^2} \right] + \dots \quad (9)$$

It can be shown that the on-shell expression (9) is gauge or BRST invariant order per order. We will have nothing to say about large gauge transformations. At the level of the off-shell or local formulation (2), the BRST invariance is explicit if one supplements the usual BRST transformation

$$\begin{aligned} s A_\mu^a &= -D_\mu^{ab} c^b, & s c^a &= \frac{g}{2} f^{abc} c^b c^c, \\ s \bar{c}^a &= i b^a, & s b^a &= 0, \end{aligned} \quad (10)$$

with the following transformations for the remaining fields:

$$s \tau^a = 0, \quad s \bar{\eta}^a = s \eta^a = 0, \quad s h^{ij} = -ig c^a (t^a)^{ik} h^{kj}. \quad (11)$$

The BRST transformation remains nilpotent ($s^2 = 0$) over the extended field space and it is immediate to check that

$$s(A^h)_\mu^a = 0, \quad (12)$$

which is nothing but the infinitesimal version of $(A_\mu^U)^{U^{-1}h} = (A_\mu^{UU^{-1}})^h = A_\mu^h$.

For later purpose, we also mention that A_μ^h becomes A_μ in the Landau gauge (at least perturbatively) as it is easily checked from (9) using $\partial_\mu A_\mu = 0$. We refer to e.g. [21–23] for more details, including the connection of the representation (9) with the (local) minimization of the ℓ_2 -norm of the gauge field.

B. BRST-invariant condensate

Having gone through this preparatory phase, we are now ready to investigate the vacuum structure of the local action $S_{\text{YM}}^{(2)} \equiv S_{\text{YM}}^{(1)} + S_1$, which is perturbatively equivalent to (1). In particular, we shall analyze the possible formation of a BRST-invariant condensate $\langle A_\mu^h A_\mu^h \rangle$. To this purpose, we couple the corresponding gluon mass operator to a source¹ J :

$$S_J^{(2)} \equiv S_{\text{YM}}^{(2)} + \int d^d x \left(Z_2 \frac{J}{2} A_\mu^h A_\mu^h - (\zeta + \delta\zeta) \mu^{-\varepsilon} \frac{J^2}{2} \right). \quad (13)$$

Here, we introduced the relevant renormalization factors and counterterms in the J -dependent piece of the action, as these will concern us most here,² next to the necessary powers of μ to ensure that $\dim \zeta = 0$ (for later use, we also note that $\dim J = 2$). More precisely, starting from bare fields, parameters and sources, which we denote by a subscript b , we write

$$J_b A_{\mu,b}^h A_{\mu,b}^h = J Z_J Z_{A_h} A_\mu^h A_\mu^h \equiv Z_2 J A_\mu^h A_\mu^h, \quad (14)$$

from which we deduce that the renormalization of the source is

$$Z_J = \frac{Z_2}{Z_{A_h}}. \quad (15)$$

Similarly,

$$\zeta_b J_b^2 \equiv (\zeta + \delta\zeta) \mu^{-\varepsilon} J^2. \quad (16)$$

The (pure vacuum) counterterm $\propto \delta\zeta J^2$ is necessary to remove the vacuum divergences in the generating

¹The method presented here was first worked out in [24]; see also [18,25,26]. We will however slightly adapt the discussion to point out some new, yet unnoticed, features, which also facilitate the interpretation.

²The other corresponding factors in $S_{\text{YM}}^{(2)}$ are tacitly assumed but not spelled out.

functional $W[J]$, with $W[J] = -\ln \int \mathcal{D} \text{fields} e^{-S_J}$, hence its appearance as an additive renormalization. Let us stress that these vacuum divergences do not affect the divergences appearing in correlation functions with at most one insertion of $A_h A_h$. Therefore, we can (and will) consider only renormalization schemes where all renormalization factors, including Z_2 , are ζ independent.

In general, from (16) it follows that

$$\begin{aligned} \mu \frac{\partial \zeta}{\partial \mu} &= -2\gamma_J \zeta + \delta, \\ \delta &= (\varepsilon - 2\gamma_J) \delta\zeta - \mu \frac{\partial \delta\zeta}{\partial \mu}, \end{aligned} \quad (17)$$

where $\mu \frac{\partial J}{\partial \mu} = \gamma_J J$. We immediately discarded terms that vanish in the $\varepsilon \rightarrow 0^+$ limit. We will recall below that, in principle, it is possible to choose $\delta\zeta$ merely proportional to ζ such that $\zeta + \delta\zeta = Z_\zeta \zeta$, henceforth implementing multiplicative renormalization also for the vacuum divergences.

We note that from (17), or directly from (16), it follows that a finite shift implies that

$$\delta\zeta \rightarrow \delta\zeta + \delta\zeta^{\text{fin}} \Rightarrow \zeta \rightarrow \zeta - \delta\zeta^{\text{fin}}, \quad (18)$$

making $\zeta + \delta\zeta$ invariant. The shift $\delta\zeta^{\text{fin}}$ can depend on all other variables. The invariance of $\zeta + \delta\zeta$ under such shifts was first discussed in [25].

From the generating functional $W[J]$, one can introduce the field

$$\sigma \equiv \frac{\delta W}{\delta J} = \frac{Z_2}{2} \langle A_\mu^h A_\mu^h \rangle_J - Z_\zeta \zeta \mu^{-\varepsilon} J, \quad (19)$$

which becomes the argument of the effective action $\Gamma(\sigma) \equiv W(J) - \int d^d x J \sigma$, with $\delta\Gamma/\delta\sigma = -J$. As usual, the benefit of such a construct is that it allows one to access the zero source limit of σ , and therefore $\langle A_\mu^h A_\mu^h \rangle_{J \rightarrow 0}$, from the minimization of $\Gamma[\sigma]$. In particular, a nontrivial minimum is tantamount to the dynamical generation of a condensate $\langle A_\mu^h A_\mu^h \rangle_{J \rightarrow 0} \neq 0$. We mention here that the nonpositivity of the integration measure associated to the action (1) could potentially jeopardize the usual relation between the limit of zero sources and the minimization of $\Gamma[\sigma]$. However, we shall later verify that the dynamically generated condensate is such that the ghost propagator remains positive, suggesting that field configurations with negative measure have a subdominant effect and, therefore, that the minimization prescription can be used. Strictly speaking, a similar check should be done with the new ghost fields η and $\bar{\eta}$.

To actually compute the effective action, it is computationally simplest to rely on Jackiw's background field method [27,28]. In the present context, this is not easily done *a priori* due to the coupling of J to a composite operator and to the presence of the quadratic term $\propto J^2$.

We can however easily remedy this situation following [18,24]. We insert a unity $1 = \mathcal{N} \int \mathcal{D}\sigma e^{-S_\sigma}$, with

$$\begin{aligned} S_\sigma &= \frac{\mu^\varepsilon}{2Z_\zeta \zeta} \int d^d x \left(\sigma - \frac{Z_2}{2} A_\mu^h A_\mu^h + Z_\zeta \zeta \mu^{-\varepsilon} J \right)^2 \\ &= \frac{\mu^\varepsilon}{2Z_\zeta \zeta} \int d^d x \left(\sigma - \frac{Z_2}{2} A_\mu^h A_\mu^h \right)^2 \\ &\quad + \int d^d x \left(J \sigma - Z_2 \frac{J}{2} A_\mu^h A_\mu^h + Z_\zeta \zeta \mu^{-\varepsilon} \frac{J^2}{2} \right). \end{aligned} \quad (20)$$

The last two terms of the third line cancel exactly the two J -dependent terms in (13) hereby defining a new sourced action

$$S_J^{(3)} = S_{\text{YM}}^{(3)} + \int d^d x J \sigma, \quad (21)$$

with $S_{\text{YM}}^{(3)} = S_{\text{YM}}^{(1)} + S_1 + S_2$, and

$$S_2 = \frac{\mu^\varepsilon}{2Z_\zeta \zeta} \int d^d x \left(\sigma^2 - Z_2 \sigma A_\mu^h A_\mu^h + \frac{Z_2^2}{4} (A_\mu^h A_\mu^h)^2 \right). \quad (22)$$

The source now couples linearly to a primary field σ [whose expectation value is of course (19)] and the background field method can be implemented as usual. Of course, integrating exactly over σ , working with $S_{\text{YM}}^{(3)}$ will give completely equivalent result as with $S_{\text{YM}}^{(2)}$. The situation will only get interesting if the dynamics of the theory would prefer to assign a nonvanishing vacuum expectation value to σ . This is a possibility that we now investigate. Before doing so, we also notice that the bare action only depends on the combination³ $\zeta + \delta\zeta$, which we already argued to be independent of the finite parts in $\delta\zeta$. Without loss of generality, we can thus renormalize the vacuum divergences in a computationally efficient scheme as $\overline{\text{MS}}$.

To do so, we first notice that, given the BRST invariance of both the action and the mass operator $A_\mu^h A_\mu^h$ as well as the fact that the α -dependent part of the action is BRST exact in the limit of zero sources, the expectation value of σ does not depend on α in this limit.⁴ Therefore, we can (and will) choose to work in the Landau gauge, $\alpha \rightarrow 0$, in which case the (τ, ξ) integration can also be done exactly, leading to the on-shell identification $A^h \rightarrow A$ [29]. At one-loop order, one obtains

³In the more general case where we would not have multiplicative renormalizability of the vacuum divergences, we simply have to replace $Z_\zeta \zeta$ by $\zeta + \delta\zeta$ in (22).

⁴The argument goes as follows:

$$\frac{d}{d\alpha} \langle \sigma \rangle_{J \rightarrow 0} \propto -i \int d^d x \langle s(A_\mu^{h,a} A_\mu^{h,a} \bar{c}^d b^d) \rangle = 0.$$

$$\begin{aligned} V(\sigma) &= \frac{\mu^{2\varepsilon} \sigma^2}{2\zeta} \left(1 - \frac{\delta\zeta}{\zeta} \right) + (N^2 - 1) \frac{d-1}{2} \mu^\varepsilon \\ &\quad \times \int_q \ln \left(q^2 - \frac{\mu^\varepsilon \sigma}{\zeta} \right), \end{aligned} \quad (23)$$

where, as usual, we have divided the effective action by the space-time volume to compute the effective potential $V(\sigma)$ and we have included an extra factor μ^ε to ensure that $\dim V = 4$. We have also treated $\delta Z_2 \equiv Z_2 - 1$ and $\delta Z_\zeta \equiv Z_\zeta - 1 = \delta\zeta/\zeta$ as higher loop corrections, neglecting them in the one-loop term and expanding to first order in $\delta\zeta$ in the tree-level term. After explicitly computing the integral and absorbing the divergence in $\delta\zeta$ using the minimal subtraction scheme, one arrives at the expression

$$V(m^2) = \zeta \frac{m^4}{2} - \frac{3(N^2 - 1)}{64\pi^2} m^4 \left[\ln \frac{\bar{\mu}^2}{m^2} + \frac{5}{6} \right], \quad (24)$$

where we have defined

$$m^2 \equiv -\mu^\varepsilon \sigma / \zeta. \quad (25)$$

C. Reduction of couplings

Various remarks are in order at this point. First, the trivial solution $m^2 = 0$ is always a maximum of the potential since $V''(m^2 \rightarrow 0) = -\infty$. This shows that, in the present approach and at the present order of evaluation, a condensate $\langle A_\mu^h A_\mu^h \rangle_{J \rightarrow 0}$ is dynamically generated (independently of the value of ζ).

Beyond this proof of existence, the next pressing question is the size of the condensate. Here, however, we face a serious problem: while the running of ζ with $\bar{\mu}$ is entirely fixed from the renormalization factor, its value at a chosen initial scale $\bar{\mu}_0$ is arbitrary and impacts directly on the size of the condensate. On the other hand, it is easily shown that $\delta W / \delta\zeta \propto \int J^2$. This means that, were we to work exactly, ζ should not influence any quantity with less than two J derivatives, in the limit of zero sources, or, in other words, at the minimum of the effective action. This includes the correlation functions for the primary fields but also the condensate itself $\langle A_\mu^h A_\mu^h \rangle_{J \rightarrow 0}$. Of course, at a given order of approximation, a spurious dependence with respect to ζ is to be expected but the previous argument shows that, given a prescription for choosing ζ , we can test *a priori* how the ζ independence (re)emerges as the approximation is improved. Let us now discuss two possible prescriptions that could be used.

A first possibility would be to impose the ζ independence of certain quantities such as the condensate or the value of the potential at the minimum. At the present order, this is not very useful because (i) the constraint does not fix any particular value of ζ and (ii) it leads to $m^2 = 0$ which we have already argued to correspond to an unstable state.

It would be interesting to see how this constraint is modified at the next order of approximation. We leave this interesting question for a future investigation.

Another possibility is to follow the prescription of [18,24]. Indeed, despite the presence of two coupling constants, g^2 and ζ , g^2 runs as usual, that is, separately from ζ . Moreover, at an exact level, the value of ζ does not affect the quantities that we are after, namely the correlation functions for the primary fields. This makes our situation suitable for the Zimmermann reduction of couplings program [19] (see also [20] for a recent overview), in which case one coupling (here ζ) is reexpressed as a series in the other (here g^2), so that the running of ζ controlled by $\gamma_\zeta(g^2)$ is then automatically satisfied. This selects one consistent coupling $\zeta(g^2)$ from a whole space of couplings ζ , and it is also the one (unique) choice compatible with multiplicative renormalizability, $\zeta + \delta\zeta = Z_\zeta \delta\zeta$. This approach was also applied to the Gross-Neveu model in [30], reporting very good agreement with the exactly known mass gap in this toy model.

In the $\overline{\text{MS}}$ scheme, one finds [3,18]

$$\zeta(g^2) = \frac{N^2 - 1}{g^2 N} \frac{9}{13} + \frac{161}{52} \frac{N^2 - 1}{16\pi^2} + \dots \equiv \frac{\zeta_0}{g^2} + \zeta_1 + \dots, \quad (26)$$

which is a particular solution of

$$\beta(g^2) \frac{\partial}{\partial g^2} \zeta(g^2) = -2\gamma_J(g^2) \zeta(g^2) + \delta(g^2), \quad (27)$$

which evidently draws from (17).

From our point of view, this choice is consistent with the perturbative approach followed in this work, where any quantity is assumed to admit an expansion (be it a Laurent expansion) in powers of g^2 .

Noticing that

$$m^2 = -\frac{g^2 \mu^\epsilon \sigma}{\zeta_0 + g^2 \zeta_1} = m_0^2 \left(1 - g^2 \frac{\zeta_1}{\zeta_0} \right), \quad (28)$$

with $m_0^2 \equiv -g^2 \mu^\epsilon \sigma / \zeta_0$, and expanding to order $\mathcal{O}(g^0)$, the potential becomes

$$\begin{aligned} V(m_0^2) &= \left(\frac{\zeta_0}{g^2} - \zeta_1 \right) \frac{m_0^4}{2} - \frac{3(N^2 - 1)}{64\pi^2} m_0^4 \left[\ln \frac{\bar{\mu}^2}{m_0^2} + \frac{5}{6} \right] \\ &= \frac{9}{13} \frac{N^2 - 1}{N} \frac{m_0^4}{2g^2} - \frac{3(N^2 - 1)}{64\pi^2} m_0^4 \left[\ln \frac{\bar{\mu}^2}{m_0^2} + \frac{113}{39} \right]. \end{aligned} \quad (29)$$

As already mentioned above, this potential admits a non-trivial minimum for $m_0^2 > 0$. Since $m_0^2 = -g^2 \sigma / \zeta_0$ with $\zeta_0 > 0$, we should then expect $\sigma < 0$. The sign is

compatible with (19) in the zero-source limit. Indeed, under the assumption that configurations beyond the Gribov horizon are negligible (which we check below), (19) implies $Z_2 \sigma \geq 0$. Moreover, since Z_2 diverges negatively [18,31], it follows that $\sigma \leq 0$ (and in practice we find $\sigma < 0$).

III. TWO-POINT FUNCTIONS

Let us now study how the dynamically generated condensate affects the Landau gauge two-point correlation functions. Rewriting the field σ in (22) as its vacuum expectation value which we also denote σ and a fluctuating part $\delta\sigma$, we find that the free gluon propagator is similar to the one in the Curci-Ferrari model:

$$D_{\mu\nu}(p) = \frac{\delta^{ab} P_{\mu\nu}^\perp(p)}{p^2 + m^2}, \quad \text{with} \quad P_{\mu\nu}^\perp(p) = \delta_{\mu\nu} - \frac{p_\mu p_\nu}{p^2}. \quad (30)$$

The ghost propagator is simply $G(p) = \delta^{ab}/p^2$, while the $\delta\sigma$ propagator is ζ/μ^ϵ . Moreover, in addition to the usual Landau gauge vertices, we have a $AA\delta\sigma$ vertex

$$\frac{\mu^\epsilon}{2\zeta} \delta^{ab} \delta_{\mu\nu} \quad (31)$$

and a new AAAA vertex

$$-\frac{\mu^\epsilon}{4! \zeta} (\delta^{ab} \delta^{cd} \delta_{\mu\nu} \delta_{\rho\sigma} + \delta^{ac} \delta^{bd} \delta_{\mu\rho} \delta_{\nu\sigma} + \delta^{ad} \delta^{bc} \delta_{\mu\sigma} \delta_{\nu\rho}). \quad (32)$$

We mention that, strictly speaking, ζ^{-1} , and therefore m^2 , have a perturbative expansion in terms of ζ_0, ζ_1, \dots which one needs to take into account in order to evaluate the correlation functions at a given order. One could define the Feynman rules in terms of this expanded parameters. However, it is more convenient, and equivalent, to consider the Feynman rules in terms of ζ^{-1} and m^2 and reexpand them only at the end of the calculation, when necessary.

A. Ghost propagator and Gribov horizon

Using the above derived Feynman rules, we find that the one-loop ghost propagator coincides with the one computed in the CF model. We can use this remark to elucidate the role of the dynamical condensate within the context of Gribov's construction [32] to avoid multiple solutions to the Landau gauge condition.

Following Gribov's original setup [32], the ambiguity related to the presence of Gribov copies is handled by restricting the domain of integration in the functional integral to the Gribov region $\Omega = \{A_\mu^a | \partial_\mu A_\mu^a = 0, \mathcal{M}^{ab}(A) > 0\}$, where \mathcal{M}^{ab} is the Faddeev-Popov operator, $\mathcal{M}^{ab} = -\partial_\mu D_\mu^{ab}$. As it is apparent from the definition of the region Ω , the ghost propagator $\langle \bar{c}^a c^b \rangle_p$, i.e., the inverse of \mathcal{M}^{ab} , remains positive within Ω . The positiveness of the

ghost propagator is thus a necessary condition for any approach to be compatible with a restriction to the Gribov region Ω , and we can check to what extent our gluon mass scale is consistent with such condition.

We parametrize the ghost two-point vertex as

$$\begin{aligned}\Gamma_{\bar{c}c}^{(2)} &= Z_c p^2 + \Sigma_{gh}(p^2) \\ &= p^2(1 - \sigma_{gh}(p^2)),\end{aligned}\quad (33)$$

where $\Sigma_{gh}(p^2) = -p^2[\sigma_{gh}(p^2) + \delta Z_c]$, with $\delta Z_c = Z_c - 1$, is the ghost self-energy and we have factored out the trivial color structure δ^{ab} . At one-loop order, one finds—modulo renormalization—

$$\sigma_{gh}(p^2) = g^2 N \frac{P_\mu P_\nu}{p^2} \int \frac{d^d q}{(2\pi)^d} \frac{P_{\mu\nu}^\perp(q)}{(p-q)^2(q^2+m^2)}, \quad (34)$$

where, to the present accuracy, m^2 can be expanded to leading order in g^2 that is replaced by m_0^2 (which we keep denoting m^2 for simplicity from here onward). As $\sigma_{gh}(p^2)$ is a decreasing function of the momentum square p^2 [33], the positivity of the ghost propagator will be ensured by demanding that $\sigma_{gh}(0) < 1$. Using dimensional regularization in the $\overline{\text{MS}}$ scheme,⁵ one finds

$$\begin{aligned}\sigma_{gh}(p^2) &= \frac{\lambda}{4} \left[-\frac{(p^2+m^2)^3}{m^2 p^4} \ln\left(\frac{p^2+m^2}{m^2}\right) \right. \\ &\quad \left. + \frac{p^2}{m^2} \ln \frac{p^2}{m^2} + \frac{m^2}{p^2} - 3 \ln \frac{m^2}{\bar{\mu}^2} + 5 \right],\end{aligned}\quad (35)$$

where we have reparametrized the coupling by defining

$$\lambda = \frac{Ng^2}{16\pi^2}. \quad (36)$$

This leads to

$$\sigma_{gh}(0) = \frac{3\lambda}{4} \left[\ln\left(\frac{\bar{\mu}^2}{m^2}\right) + \frac{5}{6} \right], \quad (37)$$

in the zero-momentum limit. The positivity condition translates then into

$$m^2 > \bar{\mu}^2 e^{\left(\frac{5}{6} - \frac{4}{3\lambda}\right)}. \quad (38)$$

On the other hand, the minimum of the potential (24) is located at

$$m^2 = \bar{\mu}^2 e^{\left(\frac{187}{78} - \frac{6}{13\lambda}\right)}. \quad (39)$$

⁵This can be checked against the more general one-loop result for $\sigma(p^2)$ derived in Sec. II B in [34], by setting there $a = \frac{1}{2}$, $v = m^2$, $w = 0$, and $b = 0$.

It is easily checked that this value obeys the positivity bound (38) for any value of λ , clarifying then the role the dynamical condensate plays in relationship to the issue of gauge copies.

B. Gluon propagator

Similarly, the gluon two-point vertex reads

$$\begin{aligned}\Gamma_{A_\mu A_\nu}^{(2)} &= Z_A p^2 P_{\mu\nu}^\perp + (1 + \delta Z_2 - \delta Z_\zeta) m^2 \delta_{\mu\nu} + [\Pi_{\text{CF},1\ell}^{m^2}]_{\mu\nu} \\ &\quad - \frac{4 \cdot 2}{2!} \left(\frac{\mu^\epsilon}{2\zeta}\right)^2 \frac{\zeta}{\mu^\epsilon} \int_Q D_{\mu\nu}(Q) \\ &\quad + \frac{4 \cdot 3}{4!} \frac{\mu^\epsilon}{\zeta} \left[\delta_{\mu\nu} \int_Q D_{\rho\rho}^{cc}(Q) + 2 \int_Q D_{\mu\nu}(Q) \right],\end{aligned}\quad (40)$$

where we have again factored out the trivial color structure δ^{ab} and it is understood that m^2 and ζ need to be expanded to the appropriate order, namely to leading order, except for the tree-level mass term m^2 that needs to be expanded to next-to-leading order according to (28). Up to the combination $Z_2 - Z_\zeta$ whose relation to the mass counterterm in the CF model we have not worked out yet, the first line is the one-loop $\Gamma_{AA}^{(2)}$ as computed in the CF model with mass m^2 . The two other contributions correspond to two new diagrams that arise from the vertices (31) and (32).

Now, the terms involving $D_{\mu\nu}$ cancel between the last two lines of (40) and we are left with

$$\begin{aligned}\Gamma_{A_\mu A_\nu}^{(2)} &= Z_A p^2 P_{\mu\nu}^\perp + (1 + \delta Z_2 - \delta Z_\zeta) m^2 \delta_{\mu\nu} + [\Pi_{\text{CF},1\ell}^{m^2}]_{\mu\nu} \\ &\quad + (N^2 - 1) \frac{d-1}{2} \frac{\mu^\epsilon}{\zeta} \delta_{\mu\nu} \int_q \frac{1}{q^2 + m^2}.\end{aligned}\quad (41)$$

Writing (23) in terms of m^2 and setting $V'(m^2) = 0$, we find

$$0 = (1 - \delta Z_\zeta) m^2 + (N^2 - 1) \frac{d-1}{2} \frac{\mu^\epsilon}{\zeta} \int_q \frac{1}{q^2 + m^2}. \quad (42)$$

This implies that

$$\Gamma_{A_\mu A_\nu}^{(2)} = Z_A p^2 P_{\mu\nu}^\perp + \delta Z_2 m^2 \delta_{\mu\nu} + [\Pi_{\text{CF},1\ell}^{m^2}]_{\mu\nu}. \quad (43)$$

For the above equation to make sense, we see that $m^2 \delta Z_2$ should correspond to the mass counterterm in the CF model $\delta m_{\text{CF}}^2 = m^2 (\delta Z_A + \delta Z_{m^2}^{\text{CF}})$. We have checked that this is indeed the case using the value for δZ_2 given in [18]. This is of course no surprise since a constant source J plays exactly the same role as the Curci-Ferrari mass and therefore $Z_J = Z_{m^2}^{\text{CF}}$, or, owing to (15), $Z_2 = Z_A Z_{m^2}^{\text{CF}}$.

Interestingly, the constant ζ disappears from the gluon self-energy [see Eq. (43)] once the latter is computed on the shell of the gap equation. This could have been foreseen, given that such a parameter was not present in

the Faddeev-Popov action in the first place; see our earlier made comments. Nonetheless, an implicit dependence on ζ still survives via the solutions of the mass gap equation.

From (43), it is evident that, although the condensate acts as a mass for the tree-level propagator, it disappears from the tree-level term at one-loop order.⁶ Thus the LCO approach does not lead to the CF model but rather to something more akin to the screened massive approach of [35–37] where the mass disappears from the loops as the order of approximation is increased. Of course, such a reorganization of the perturbative expansion does not necessarily lead to a trivial reformulation of the theory without condensates. In this respect, it would be interesting to push the present approach to the next order and identify quantities that remain constant and different from their corresponding predictions in the absence of condensate. We leave this interesting question for future work. Nonetheless, in Appendix B we already offer a generic argument as to why the tree-level mass indeed should cancel upon using the gap equation.

C. The dynamically infrared-safe scheme and the renormalization group

We would now like to compare our results to lattice data. To this purpose, we need to choose a renormalization scheme that is free of Landau poles and that yields a gluon propagator which displays the desired infrared behavior. The renormalization factors we need to fix are Z_A , Z_c , Z_λ and Z_2 . We will also redefine Z_ζ to better match our scheme, rather than using $\overline{\text{MS}}$ like we did in Sec. II B. Since Z_ζ ultimately only affects the solution to the gap equation, we will postpone this to the next section.

To begin with, since we are in the Landau gauge, in order to fix the coupling renormalization Z_λ we can impose the Taylor condition

$$Z_\lambda Z_A Z_c^2 = 1. \quad (44)$$

In the Taylor scheme, the running of λ is completely determined by the anomalous dimensions γ_A and γ_c of the gluon and ghost propagators:

$$\beta_\lambda = \mu \frac{d\lambda}{d\mu} = -\mu \frac{d \ln Z_\lambda}{d\mu} \lambda = \lambda(\gamma_A + 2\gamma_c), \quad (45)$$

⁶Strictly speaking, the gluon propagator is obtained after considering $\Gamma_{A\delta\sigma}^{(2)}$, $\Gamma_{\delta\sigma A}^{(2)}$ and $\Gamma_{\delta\sigma\delta\sigma}^{(2)}$ and inverting

$$\Gamma_{AA}^{(2)} - \Gamma_{A\delta\sigma}^{(2)} [\Gamma_{\delta\sigma\delta\sigma}^{(2)}]^{-1} \Gamma_{\delta\sigma A}^{(2)}.$$

Fortunately, using that $\zeta^{-1} \sim g^2$, it is easily shown, however, that $\Gamma_{A\delta\sigma}^{(2)} \sim \Gamma_{\delta\sigma A}^{(2)} \sim g^3$ while $\Gamma_{\delta\sigma\delta\sigma}^{(2)} \sim g^2$ which means that the extra term can be neglected at the present order of accuracy. We also note that $\Gamma_{A\delta\sigma}^{(2)}$ vanishes in the zero-momentum limit from symmetry considerations.

where

$$\gamma_A = \frac{d \ln Z_A}{d \ln \mu}, \quad \gamma_c = \frac{d \ln Z_c}{d \ln \mu}. \quad (46)$$

Z_A and Z_c themselves can be defined in the momentum subtraction (MOM) scheme, as is appropriate for a comparison with the lattice data. Namely, if we renormalize the gluon and ghost propagators at the scale μ so that

$$\Gamma_{AA}^{(2)\perp}(p^2 = \mu^2) = \Gamma_{cc}^{(2)}(p^2 = \mu^2) = \mu^2 \quad (47)$$

(here $\Gamma_{AA}^{(2)\perp}$ denotes the transverse component of the gluon two-point vertex), then, going back to (43) and (33),

$$Z_A = 1 - \delta Z_2 \frac{m^2}{\mu^2} - \frac{\Pi_{\text{CF},1\ell}^{m^2\perp}(p^2 = \mu^2)}{\mu^2}, \quad (48)$$

$$Z_c = 1 - \frac{\Sigma_{gh}(p^2 = \mu^2)}{\mu^2}, \quad (49)$$

where $\Pi_{\text{CF},1\ell}^{m^2\perp}$ is the transverse component of the CF gluon polarization [5]:

$$\begin{aligned} \Pi_{\text{CF},1\ell}^{m^2\perp}(\mu^2) = & -\frac{\lambda m^2}{6} \left(13t - \frac{9}{2} \right) \left(\frac{2}{\epsilon} + \ln \frac{\bar{\mu}^2}{m^2} \right) \\ & - \frac{\lambda m^2}{24t^2} \left[\frac{242}{3} t^3 - 126t^2 + 2t + (t^2 - 2)t^3 \ln t \right. \\ & - 2(t+1)^3(t^2 - 10t + 1) \ln(t+1) \\ & \left. - t^{3/2}(t+4)^{3/2}(t^2 - 20t + 12) \right. \\ & \left. \times \ln \left(\frac{\sqrt{t+4} - \sqrt{t}}{\sqrt{t+4} + \sqrt{t}} \right) \right], \quad (50) \end{aligned}$$

with $t = \mu^2/m^2$. Observe that the first of the conditions in (47) is especially suitable to our model, which does not have a tree-level mass term in the inverse propagator. Indeed, due to the cancellations which occur in (41) as soon as the gap equation is enforced, (47) is favored over conditions such as $\Gamma_{AA}^{(2)\perp}(\mu^2) = \mu^2 + m^2$, which is often used for renormalizing the gluon propagator in the CF model [5].

At this stage, δZ_2 in (48) remains yet undetermined. Before discussing its definition, let us explore how Z_2 is relevant to renormalization, starting from the gluon mass m^2 . In the present model, we do not really have a mass renormalization factor since $m^2 = -g^2 \sigma / \zeta_0$ is defined only at the renormalized level. This is at variance with the CF model, where it is found [4,5,26] that $\beta_{m^2} = m^2(\gamma_A + \gamma_c)$. However, we can rewrite m^2 in terms of μ -independent bare quantities modulo μ -dependent renormalization factors. Explicitly, we have

$$m^2 = -\frac{g^2 \bar{\mu}^\epsilon}{2\zeta_0} Z_2 \langle A^2 \rangle = -\frac{g_b^2 \bar{\mu}^\epsilon}{2\zeta_0} \frac{Z_2}{Z_\lambda Z_A} \langle A_b^2 \rangle. \quad (51)$$

It follows that the μ dependence of m^2 is encoded in the prefactor

$$\frac{Z_2}{Z_\lambda Z_A} = Z_2 Z_c^2, \quad (52)$$

where we have used the Taylor condition (44). In particular, the μ dependence of m^2 is entirely governed by Z_2 and Z_c , with the square mass beta function β_{m^2} reading

$$\beta_{m^2} = \mu \frac{dm^2}{d\mu} = m^2(\gamma_2 + 2\gamma_c). \quad (53)$$

Furthermore, as we have seen in Sec. II B, Z_2 plays the same role as $Z_A Z_m^{\text{CF}}$ in the CF model. Since the latter enjoys a non-nilpotent BRST symmetry which implies that $Z_m^{\text{CF}} Z_A Z_c$ is UV finite, we deduce that, in the present model, $Z_2 Z_c$ should also be UV finite.⁷ The most obvious condition to impose for defining Z_2 would then be $Z_2 Z_c = 1$ [26]. However, there are good reasons to use a slightly different definition.

To see why an alternative condition to $Z_2 Z_c = 1$ is appropriate in the present renormalization scheme, it is instructive to compute the low-energy limit of the beta function β_λ while keeping δZ_2 arbitrary. As $\mu^2 \rightarrow 0$, we have—see Eqs. (35), (37), and (50)—

$$\Pi_{\text{CF},1\ell}^{m^2\perp}(\mu^2) = \frac{3\lambda m^2}{4} \left(\frac{2}{\epsilon} + \frac{5}{6} + \ln \frac{\bar{\mu}^2}{m^2} \right) + O(\mu^2), \quad (54)$$

$$\Sigma_{gh}(\mu^2) = -\frac{3\lambda \mu^2}{4} \left(\frac{2}{\epsilon} + \frac{5}{6} + \ln \frac{\bar{\mu}^2}{m^2} \right) + O(\mu^4), \quad (55)$$

where the $O(\mu^2)$ term in $\Pi_{\text{CF},1\ell}^{m^2\perp}$ contains a logarithm of μ^2 . Plugging these into (48) and (49) and using (46) while neglecting any higher-order term in the renormalization scale and in the coupling, we find that the gluon and ghost anomalous dimensions have the following asymptotic behavior:

$$\gamma_A = \left[2\delta Z_2 + \frac{3\lambda}{2} \left(\frac{2}{\epsilon} + \frac{5}{6} + \ln \frac{\bar{\mu}^2}{m^2} \right) \right] \frac{m^2}{\mu^2} + O(\mu^0), \quad (56)$$

$$\gamma_c = O(\mu^2). \quad (57)$$

By (45), these yield

⁷This can also be seen either by an explicit calculation starting from (48) and (49) or from the fact that a constant source J plays the role of the square mass in the Curci-Ferrari model and therefore $Z_J = Z_2/Z_A = Z_m^{\text{CF}}$.

$$\beta_\lambda = \left[2\delta Z_2 + \frac{3\lambda}{2} \left(\frac{2}{\epsilon} + \frac{5}{6} + \ln \frac{\bar{\mu}^2}{m^2} \right) \right] \frac{\lambda m^2}{\mu^2} + O(\mu^0). \quad (58)$$

For most values of δZ_2 , subject to the sole condition that γ_A (or, equivalently, β_λ) do not contain divergences, we find that

$$\mu \frac{d\lambda}{d\mu} \propto \frac{\lambda^2 m^2}{\mu^2} (\mu \rightarrow 0), \quad (59)$$

which is equivalent to⁸

$$\lambda(\mu) \propto \frac{\mu^2}{m^2} \rightarrow 0 (\mu \rightarrow 0). \quad (60)$$

This behavior is consistent with the one found for the Taylor coupling on the lattice [38]. On the other hand, suppose that $\delta Z_2 = -\delta Z_c$, as would be the case to one loop if we decided to choose our renormalization condition according to $Z_2 Z_c = 1$. Then we would have, by (49) and (55),

$$\delta Z_2 = -\delta Z_c = -\frac{3\lambda}{4} \left(\frac{2}{\epsilon} + \frac{5}{6} + \ln \frac{\bar{\mu}^2}{m^2} \right) + O(\mu^2), \quad (61)$$

yielding $\beta_\lambda \rightarrow \text{constant} \times \lambda^2$ in the low-energy limit. This is equivalent to $\lambda(\mu) \propto 1/\ln \mu^2 \rightarrow 0$ as $\mu \rightarrow 0$.

While having a running coupling that vanishes logarithmically at zero momentum might not be an issue in and of itself, if we insist that $Z_2 Z_c = 1$ in the Taylor scheme, then we run into the conclusion that the gluon propagator remains massless at low energy, when improved by the methods of the renormalization group (RG). In order to see this, let us first write down the explicit expression for the RG-improved gluon two-point vertex in the present scheme. Denoting by $\Gamma_{AA}^{(2)\perp}(p; \mu)$ the two-point vertex renormalized by minimal subtraction at the scale μ , one has

$$\Gamma_{AA}^{(2)\perp}(p; \mu) = p^2 \exp \left\{ - \int_\mu^p \frac{d\tilde{\mu}}{\tilde{\mu}} \gamma_A(\tilde{\mu}) \right\}. \quad (62)$$

As already observed in [39] based on the relation $m^2 \propto g^2 \langle A^2 \rangle$, $Z_2 Z_c = 1$ implies $\gamma_2 = -\gamma_c$, so that, by (53),

$$\beta_{m^2} = \gamma_c m^2. \quad (63)$$

The gluon anomalous dimension γ_A can then be rewritten as

$$\gamma_A = \frac{\beta_\lambda}{\lambda} - 2 \frac{\beta_{m^2}}{m^2}, \quad (64)$$

where in deriving the above equality we used the Taylor condition. We then compute

⁸Here we are assuming that m^2 does not vanish as $\mu \rightarrow 0$. As we will see later on, this is indeed the case.

$$\begin{aligned} \int_{\mu}^p \frac{d\tilde{\mu}}{\tilde{\mu}} \gamma_A(\tilde{\mu}) &= \int_{\mu}^p d\tilde{\mu} \left(\frac{1}{\tilde{\mu}} \frac{d\lambda}{d\tilde{\mu}} - \frac{2}{m^2} \frac{dm^2}{d\tilde{\mu}} \right) \\ &= \ln \left(\frac{\lambda(p) m^4(p)}{\lambda(\mu) m^4(\mu)} \right). \end{aligned} \quad (65)$$

Our final expression for the RG-improved gluon two-point vertex therefore reads

$$\Gamma_{AA}^{(2)\perp}(p; \mu) = p^2 \frac{\lambda(\mu) m^4(p)}{\lambda(p) m^4(\mu)}. \quad (66)$$

We remark that this expression is valid in any scheme in which $\gamma_2 = -\gamma_c$ holds together with the Taylor condition.

Now, since according to (57) (and by dimensional counting)

$$\gamma_c(\mu) \propto \lambda \frac{\mu^2}{m^2} \quad (\mu \rightarrow 0), \quad (67)$$

using $\beta_{m^2} = \gamma_c m^2$, we find that

$$\mu \frac{dm^2}{d\mu} \propto \lambda \mu^2 \quad (\mu \rightarrow 0). \quad (68)$$

Provided that the running coupling vanishes at zero momentum (whether logarithmically or quadratically is irrelevant), the above equation implies that $m^2(\mu)$ saturates to a constant in the low-energy limit. Therefore, as $p \rightarrow 0$, we find that

$$\Gamma_{AA}^{(2)\perp}(p; \mu) \sim \frac{p^2}{\lambda(p)} \quad (p \rightarrow 0). \quad (69)$$

We now see why having a logarithmically vanishing coupling spoils the infrared behavior of the RG-improved gluon propagator: if $\lambda(p) \sim 1/\ln p^2$, then $\Gamma_{AA}^{(2)\perp}(p) \sim p^2 \ln p^2$, implying that the propagator diverges at $p = 0$.

Ultimately, the reason why we found this divergence is that the specific choice $Z_2 Z_c = 1$, which to one loop is equivalent to $\delta Z_2 = -\delta Z_c$, kills the deep-infrared m^2/μ^2 term in the beta function β_λ . Using such a condition, however, is not at all forced on us by any consistency requirement: so long as the divergences in δZ_2 and δZ_c are taken to be equal with an opposite sign, we are free to choose the finite part of Z_2 according to the needs of our scheme. Therefore, instead of picking the single value that yields a diverging propagator, we decide to use a slightly different renormalization condition for δZ_2 , namely

$$\delta Z_2 = -\delta Z_c + \lim_{\mu \rightarrow 0} [\delta Z_c]_{\text{fin}}, \quad (70)$$

where $[\delta Z_c]_{\text{fin}}$ is the finite part of δZ_c . In other words, we start from δZ_c and subtract from it its zero-energy finite term. Note that in the MOM scheme any $\tilde{\mu}$ -dependent term

must actually be regarded as part of the divergence, since $\tilde{\mu}$ is an arbitrary scale introduced by dimensional regularization which needs to be absorbed by renormalization.

Going back to (61), we see that, to leading order, the above condition is equivalent to

$$\delta Z_2 = -\delta Z_c + \frac{5\lambda}{8} \quad \text{or} \quad Z_2 Z_c = 1 + \frac{5\lambda}{8}. \quad (71)$$

Immediately, we find that in the scheme defined by (70), which henceforth we will refer to as the dynamically infrared-safe (DIS) scheme, the beta function β_λ regains its infrared m^2/μ^2 term:

$$\beta_\lambda = \frac{5\lambda^2 m^2}{4 \mu^2} + O(\mu^2). \quad (72)$$

As discussed earlier, this implies that λ vanishes quadratically as $\mu \rightarrow 0$. Furthermore, since the difference between δZ_2 and $-\delta Z_c$ is a μ -independent constant, the relation $\gamma_2 = -\gamma_c$ still holds despite being $Z_2 Z_c \neq 1$. Therefore, the expression in (66) for the RG-improved gluon two-point vertex is still valid in the DIS scheme, as well as the asymptotic behavior described by (69). However, this time $\lambda(p) \sim p^2$, so that

$$\Gamma_{AA}^{(2)\perp}(p; \mu) \rightarrow \text{const}(p \rightarrow 0) \quad (73)$$

and the propagator saturates to a constant at zero momentum, as it should be.

In the present scheme, the gluon and ghost anomalous dimensions γ_A and γ_c read, respectively,

$$\begin{aligned} \gamma_A &= -\frac{\lambda}{6t^3} \left[17t^3 - \frac{163}{2}t^2 + 12t - t^5 \ln t \right. \\ &\quad \left. + (2t-3)(t-2)^2(t+1)^2 \ln(t+1) \right. \\ &\quad \left. + t^{3/2} \sqrt{t+4} (t^3 - 9t^2 + 20t - 36) \ln \left(\frac{\sqrt{t+4} - \sqrt{t}}{\sqrt{t+4} + \sqrt{t}} \right) \right], \end{aligned} \quad (74)$$

$$\gamma_c = -\frac{\lambda}{2t^2} [2t^2 + 2t - t^3 \ln t + (t-2)(t+1)^2 \ln(t+1)], \quad (75)$$

where $t = \mu^2/m^2$. In the UV, the ordinary Yang-Mills behavior, namely

$$\gamma_A \rightarrow -\frac{13\lambda}{3}, \quad \gamma_c \rightarrow -\frac{3\lambda}{2} \quad (\mu \rightarrow \infty), \quad (76)$$

is recovered. As we will see, the RG-improved gluon and ghost propagators computed from these anomalous dimensions are in very good agreement with the lattice data over a wide range of momenta.

Finally, let us write down an expression analogous to (66) for the RG-improved ghost two-point vertex. In general, the two-point vertex $\Gamma_{\bar{c}c}^{(2)}(p; \mu)$ renormalized by minimal subtraction at the scale μ can be written as

$$\Gamma_{\bar{c}c}^{(2)}(p; \mu) = p^2 \exp \left\{ - \int_{\mu}^p \frac{d\tilde{\mu}}{\tilde{\mu}} \gamma_c(\tilde{\mu}) \right\}. \quad (77)$$

Since in our scheme $\gamma_c = \beta_{m^2}/m^2$, we compute

$$\begin{aligned} \int_{\mu}^p \frac{d\tilde{\mu}}{\tilde{\mu}} \gamma_c(\tilde{\mu}) &= \int_{\mu}^p d\tilde{\mu} \frac{1}{m^2} \frac{dm^2}{d\tilde{\mu}} \\ &= \ln \left(\frac{m^2(p)}{m^2(\mu)} \right). \end{aligned} \quad (78)$$

In particular, the ghost two-point vertex can be expressed in terms of the running gluon mass squared $m^2(p)$ as

$$\Gamma_{\bar{c}c}^{(2)}(p; \mu) = p^2 \frac{m^2(\mu)}{m^2(p)}. \quad (79)$$

The above equation tells us that the ghost propagator diverges like $1/p^2$ at zero momentum and that the ghost form factor—as a function of momentum—has the same behavior as the running gluon mass squared, being essentially equal to it modulo a constant factor of $m^{-2}(\mu)$.

In the next section, we will redefine the gap equation in order to derive suitable initial conditions for the RG flow of the theory. These will be used to compute the RG-improved gluon and ghost propagators, which we will then compare with the lattice data in a later section.

D. Gap equation revisited and the RG flow

The gap equation allows us to fix the initial value of the gluon mass m^2 in the RG flow starting from the initial renormalization scale μ and coupling λ . Analogously as for the propagators, we will benefit from the RG invariance of the effective potential (29) to optimize it. We can first work in the $\overline{\text{MS}}$ scheme to do so. As per construction $\bar{\mu} \frac{d}{d\bar{\mu}} V = 0$, or,

$$\left(\bar{\mu} \frac{\partial}{\partial \bar{\mu}} + \beta(g^2) \frac{\partial}{\partial g^2} + \beta_{m^2}(g^2) \frac{\partial}{\partial m^2} \right) V = 0, \quad (80)$$

we can use this RG equation to resum all leading logs. Therefore, we set

$$V_{LL}(m) = \frac{9}{13} \frac{N^2 - 1}{N} \frac{m^4}{2g^2} \sum_{n=0}^{\infty} v_n u^n, \quad (81)$$

with $v_0 = 1$ and $u = g^2 \ln(m^2/\bar{\mu}^2)$. Setting $\beta(g^2) = -2g^2 \sum_{n=0}^{\infty} \beta_n(g^2)^{n+1}$ and $\beta_{m^2}(g^2)/m^2 = g^2 \sum_{n=0}^{\infty} \gamma_n(g^2)^n$, we get from (80) at leading order

$$(\gamma_0 + \beta_0) \sum_{n=0}^{\infty} v_n u^n - (\beta_0 u + 1) \sum_{n=0}^{\infty} (n+1) v_{n+1} u^n = 0. \quad (82)$$

This can be rephrased as

$$(\gamma_0 + \beta_0)F(u) - (\beta_0 u + 1)F'(u) = 0 \quad (83)$$

with $F(u) = \sum_{n=0}^{\infty} v_n u^n$. Using $v_0 = 1$, the solution reads

$$F(u) = (1 + \beta_0 u)^{1+\gamma_0/\beta_0}, \quad (84)$$

and the optimized potential becomes

$$V_{LL}(m) = \frac{9}{13} \frac{N^2 - 1}{N} \frac{m^4(\bar{\mu})}{2g^2(\bar{\mu})} \left(1 + \beta_0 g^2(\bar{\mu}) \ln \frac{m^2(\bar{\mu})}{\bar{\mu}^2} \right)^{1+\gamma_0/\beta_0}. \quad (85)$$

The above RG methodology was borrowed from [40]; see also [41] for further interesting comments about RG log resummations. In Appendix C, we have taken a closer look at the effective potential.

It can be easily seen that at this order, the last factor amounts to replacing $\frac{m^4(\bar{\mu})}{2g^2(\bar{\mu})} \rightarrow \frac{m^4(m)}{2g^2(m)}$, clearly showing potentially large logs are resummed, and thereby also establishing the explicit $\bar{\mu}$ independence of the improved effective potential; see also [41].

Expressing everything in terms of λ , we obtain as solution of $\frac{\partial V_{LL}}{\partial m} = 0$ in the $\overline{\text{MS}}$ scheme

$$m_{\text{sol},\overline{\text{MS}}}(\bar{\mu}) = \bar{\mu} e^{-\frac{13}{88} - \frac{3}{22\overline{\text{MS}}(\bar{\mu})}}, \quad (86)$$

as $\beta_0 = \frac{11N}{3(16\pi^2)}$ and $\gamma_0 = -\frac{3N}{2(16\pi^2)}$; see e.g. [3] and (63). For later usage in Appendix C, we already mention $\beta_1 = \frac{34N^2}{3(16\pi^2)^2}$ and $\gamma_1 = -\frac{95N^2}{24(16\pi^2)^2}$.

In order to make use of this solution in the DIS scheme, we first need to perform a scheme conversion from $\overline{\text{MS}}$ to DIS, using the appropriate renormalization factors. Going back to (44) and (52) we see that, at a fixed renormalization scale,

$$m_{\text{DIS}}^2 = \frac{Z_{2,\text{DIS}} Z_{c,\text{DIS}}^2}{Z_{2,\overline{\text{MS}}} Z_{c,\overline{\text{MS}}}^2} m_{\overline{\text{MS}}}^2, \quad (87)$$

$$\lambda_{\text{DIS}} = \frac{Z_{A,\text{DIS}} Z_{c,\text{DIS}}^2}{Z_{A,\overline{\text{MS}}} Z_{c,\overline{\text{MS}}}^2} \lambda_{\overline{\text{MS}}}, \quad (88)$$

or, to one loop, since $Z_{2,\overline{\text{MS}}} Z_{c,\overline{\text{MS}}} = 1$,

$$m_{\text{DIS}}^2 = \left[1 + \frac{5\lambda}{8} + (\delta Z_{c,\text{DIS}} - \delta Z_{c,\overline{\text{MS}}}) \right] m_{\overline{\text{MS}}}^2, \quad (89)$$

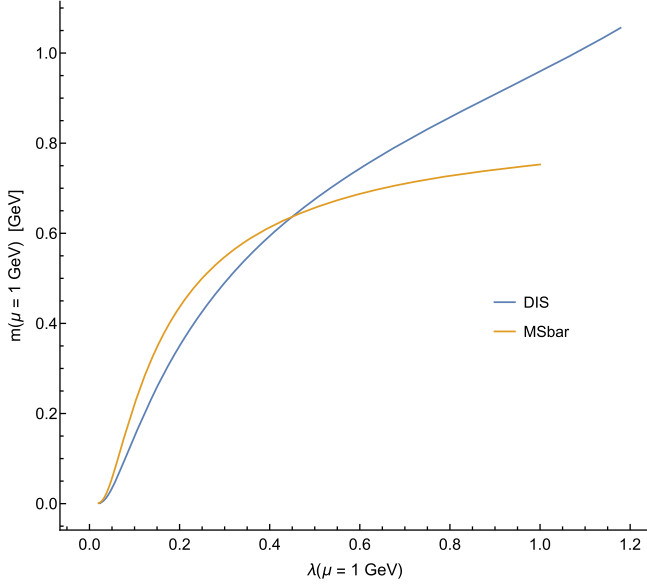


FIG. 1. Solutions of the gap equation in the DIS and $\overline{\text{MS}}$ schemes at the renormalization scale $\mu_0 = 1$ GeV.

$$\lambda_{\text{DIS}} = [1 + (\delta Z_{A,\text{DIS}} - \delta Z_{A,\overline{\text{MS}}}) + 2(\delta Z_{c,\text{DIS}} - \delta Z_{c,\overline{\text{MS}}})] \lambda_{\overline{\text{MS}}}. \quad (90)$$

Of course, to lowest order, the mass and coupling on which the renormalization factors depend can be computed in any of the two schemes.

In what follows, we will fix the renormalization scale to be equal to $\mu_0 = 1$ GeV—i.e., the scale at which we start the renormalization group flow—and use $\lambda_{\text{DIS}}(\mu_0)$ as our independent variable. Then we will compute $\lambda_{\overline{\text{MS}}}(\mu_0)$ as a function of $\lambda_{\text{DIS}}(\mu_0)$ using (90), plug the result into (86) to obtain the solution of the $\overline{\text{MS}}$ resummed gap equation, and finally convert the solution to the DIS scheme using (89). Doing so yields the DIS mass $m_{\text{DIS}}^2(\mu_0)$ corresponding to the DIS coupling $\lambda_{\text{DIS}}(\mu_0)$ by virtue of the $\overline{\text{MS}}$ gap equation. In Fig. 1 we show the solutions of the gap equation, both in the $\overline{\text{MS}}$ and in the DIS scheme, at the scale $\mu_0 = 1$ GeV. As we can see, the conversion modifies only slightly the relation between the mass and coupling, at least for not so large values of λ .

Dropping the subscript for the DIS quantities, with the DIS $m_0 = m(\mu_0) = m_{\text{sol}}$ computed at the initial scale μ_0 as a function of the DIS coupling $\lambda_0 = \lambda(\mu_0)$ as detailed above, in Fig. 2 we display some of the solutions to the beta-function equations in the DIS scheme. As we can see, the running coupling has no infrared Landau pole⁹ and vanishes like p^2 as $p \rightarrow 0$, as we anticipated in the last section. The absence of Landau poles in the running coupling is a necessary condition for the self-consistency

⁹We checked that this behavior persists to very large values of the coupling λ_0 at the initial scale $\mu_0 = 1$ GeV. Indeed, we could not find any value of λ_0 for which the running coupling diverges.

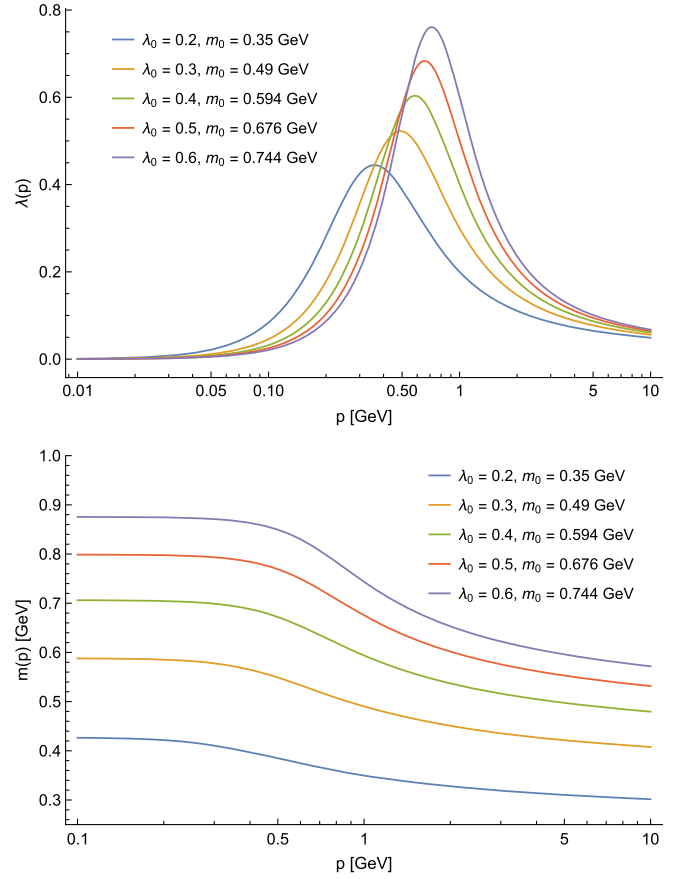


FIG. 2. DIS running coupling (top) and mass (bottom) for different values of the coupling λ_0 at the initial scale $\mu_0 = 1$ GeV, with the corresponding mass m_0 computed by solving the gap equation.

of any perturbative approach to quantum chromodynamics and one which is shared by most of the models which treat the gluons as massive—see e.g. [10,37]. Indeed, it is precisely the existence of a gluon mass scale that makes it possible for the running coupling to change its behavior and decrease as the momentum decreases. At large energies, since $\beta_\lambda \rightarrow -\frac{22\lambda^2}{3}$ as $\mu \rightarrow \infty$ by (74) and (75), the coupling runs just like in ordinary Yang-Mills theory.

Finally, at zero momentum the running gluon mass saturates to a constant $m(0)$, again in agreement with our analysis of Sec. III C. Since $\beta_{m^2} < 0$, with $m_0 = m_{\text{sol}}$ an increasing function of λ_0 , $m(0)$ increases with the initial value of the coupling. It attains the expected order of magnitude when $\lambda_0 \gtrsim 0.2$ – 0.3 , which corresponds to values of the coupling $\lambda \gtrsim 0.4$ – 0.5 at the peak (equivalently, $\alpha_s \gtrsim 1.7$ – 2.1). In the UV, we find that

$$\beta_{m^2} \rightarrow -\frac{3\lambda m^2}{2} \quad (\mu \rightarrow \infty), \quad (91)$$

yielding a mass that decreases like $\lambda^{\frac{9}{44}}(\mu) \sim [\ln(\mu^2)]^{-\frac{9}{44}}$ at large energies, thereby restoring the massless, asymptotically free, UV limit.

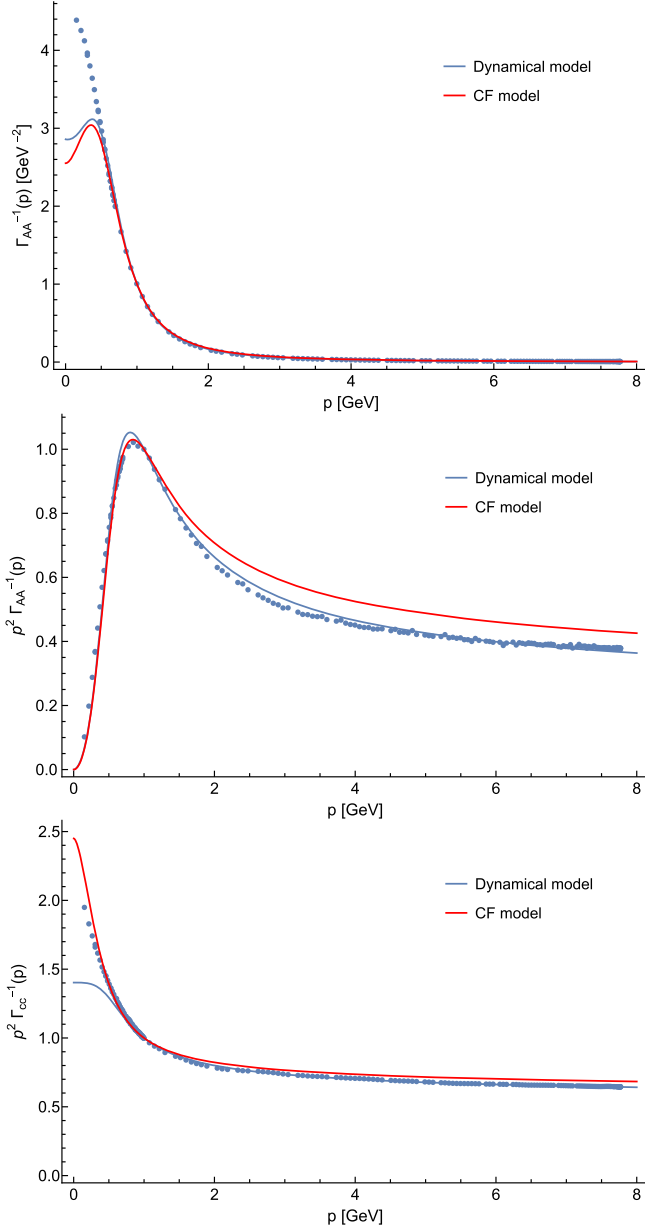


FIG. 3. RG-improved gluon propagator (top), gluon form factor (middle) and ghost form factor (bottom) in the DIS scheme, renormalized at $\mu_0 = 1$ GeV, together with the lattice data of [38] and analogous CF model results (red curves) for comparison; see the text for details. The initial value of the coupling $\lambda_0 = 0.473$ was obtained by fitting the combined lattice data for the gluon and ghost form factors. The initial value of the gluon mass $m_0 = 0.655$ GeV was computed by using the gap equation as described in Sec. III D.

E. Comparison with the lattice data

We are now in a position to compare the predictions of our model with the lattice data, more precisely the 80^4 , $\beta = 6.0$ gluon and ghost datasets of [38]; see also [42]. In Fig. 3 we show the RG-improved gluon propagator, gluon form factor and ghost form factor renormalized at the scale

$\mu_0 = 1$ GeV. In order to obtain the two-point functions, we fitted the initial value of the coupling¹⁰ by the least-squares method using the combined lattice data of [38] for the gluon and ghost form factors, with the gluon mass $m_0 = m_{\text{sol}}$ computed from the gap equation as a dependent input, as described in the previous section. The fit yielded a value of $\lambda_0 = 0.473$, which corresponds to $\alpha_s(\mu_0) = 1.981$, $m_0 = 0.655$ GeV, and $\lambda_{\overline{\text{MS}}}(\mu_0) = 0.316$.

Both the form factors turn out to be in very good agreement with the lattice data at moderate to high energies—up to 8 GeV—despite the gluon falling slightly below the lattice in the UV and slightly above it at intermediate energies. On the other hand, at momenta $p \lesssim 0.5$ GeV, the RG-improved functions are suppressed with respect to their lattice analogs. This behavior is not unseen at one loop in massive expansions of Yang-Mills theory [43], at least as far as the gluon is concerned. Indeed, it is shown by the CF model itself, when the latter is fitted to the lattice data by the same procedure used for our fit.¹¹ Previous studies of the CF model [8] suggest that this behavior could improve by going to two loops.

The running coupling $\lambda(p)$ and mass $m(p)$ given the initial value $\lambda_0 = 0.473$ and the gap equation are shown in Fig. 4. The maximum of the coupling occurs at $p \approx 0.64$ GeV, where $\lambda \approx 0.66$ (i.e., $\alpha_s \approx 2.77$). At zero momentum, the running mass saturates to $m(0) \approx 0.78$ GeV.

In Fig. 5 we compare the lattice data for the Taylor coupling to our running coupling $\alpha_s(p)$. Since the fitted λ_0 [equivalently, $\alpha_s(\mu_0)$] is a one-loop estimate of the coupling, a rescaling of $\alpha_s(p)$ is needed in order to match the lattice. In our case, we had to divide $\alpha_s(p)$ by 2.2 in order to align the former both to the lattice UV tail and to the value of α_s at the initial renormalization scale μ_0 . At $\mu_0 = 1$ GeV, the rescaled value of the coupling α_s is found to be 0.90.

F. Testing the stability of the DIS scheme

In order to test the stability of the DIS scheme, it is useful to extend the results presented in Secs. III C–III E to different initial renormalization scales μ_0 and to alternative renormalization parameters.

For the purposes of this section, we shall denote with ΔZ the quantity defined as

¹⁰In order to simplify the numerical calculations, we used the $\overline{\text{MS}}$ coupling $\lambda_{\overline{\text{MS}}}(\mu_0)$ at μ_0 as the fit parameter and then obtained the DIS scheme λ_0 using Eqs. (86) and (90).

¹¹We should remark that the CF fit shown in Fig. 3 is not part of the original studies on the subject, but rather it was made anew starting from the combined gluon and ghost lattice form factors of [38] for the purpose of comparison. In more detail, the RG-improved CF functions were computed in the so-called infrared-safe scheme [5], rescaled so that $\Gamma_{AA}^{(2)\perp}(p)/p^2 = 1$ at $p = 1$ GeV, like in our DIS scheme. The rescaling factor could as well be determined by leaving it as a free parameter of the fit, in which case the CF propagators would significantly improve—especially in the UV. However, we chose not to do so, in order to make the comparison to our results more immediate.

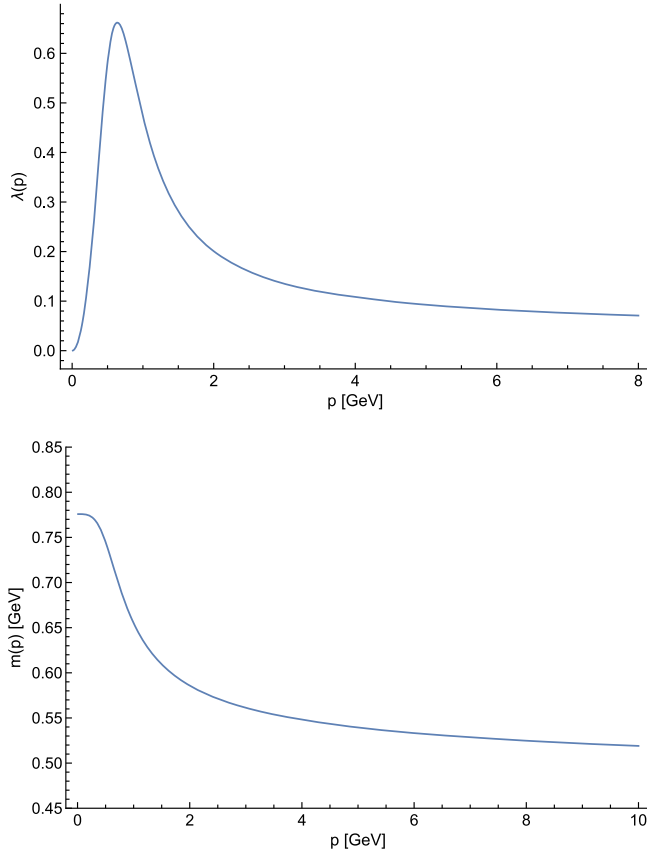


FIG. 4. Running coupling (top) and mass (bottom) corresponding to the fit in Fig. 3.

$$\Delta Z = Z_2 Z_c - 1. \quad (92)$$

In our previous analysis, we took $\Delta Z = \frac{5\lambda}{8}$, the latter being equal to the one-loop zero-momentum limit of the finite part of δZ_c . While natural in many respects, this choice is far from unique: in Sec. III C we saw that any nonzero ΔZ of the form $\text{const} \times \lambda$ yields a gluon propagator which

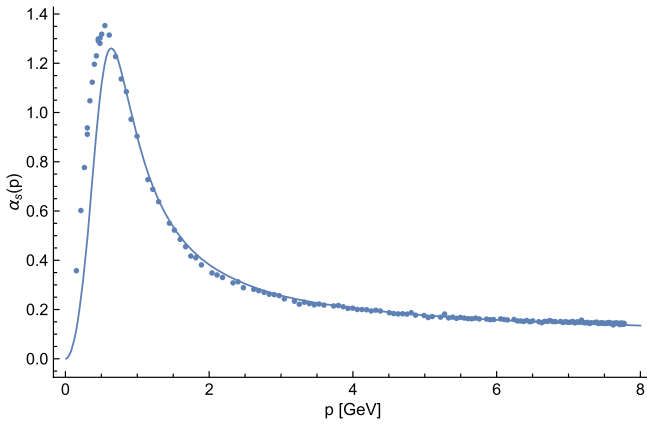


FIG. 5. Running coupling corresponding to the fit in Fig. 3, rescaled by a factor of 1/2.2. Lattice data from [38]. See the text for details.

saturates to a finite value as $p \rightarrow 0$. It thus makes sense to ask whether choosing a constant other than 5/8 in ΔZ would substantially alter our results.

In Figs. 6 and 7 we answer this question by fitting the lattice data while setting $\Delta Z = \frac{5\lambda}{8} \pm 20\%$ —that is, $\Delta Z = \frac{\lambda}{2}, \frac{3\lambda}{4}$. Additionally, we integrate the RG flow starting from three different initial renormalization scales— $\mu_0 = 1, 2$ and 5 GeV—in order to test the scale dependence of the scheme. The fit parameters—reported in Table I—were obtained by adapting the procedure laid out in Secs. III D and III E to the new renormalization parameters.

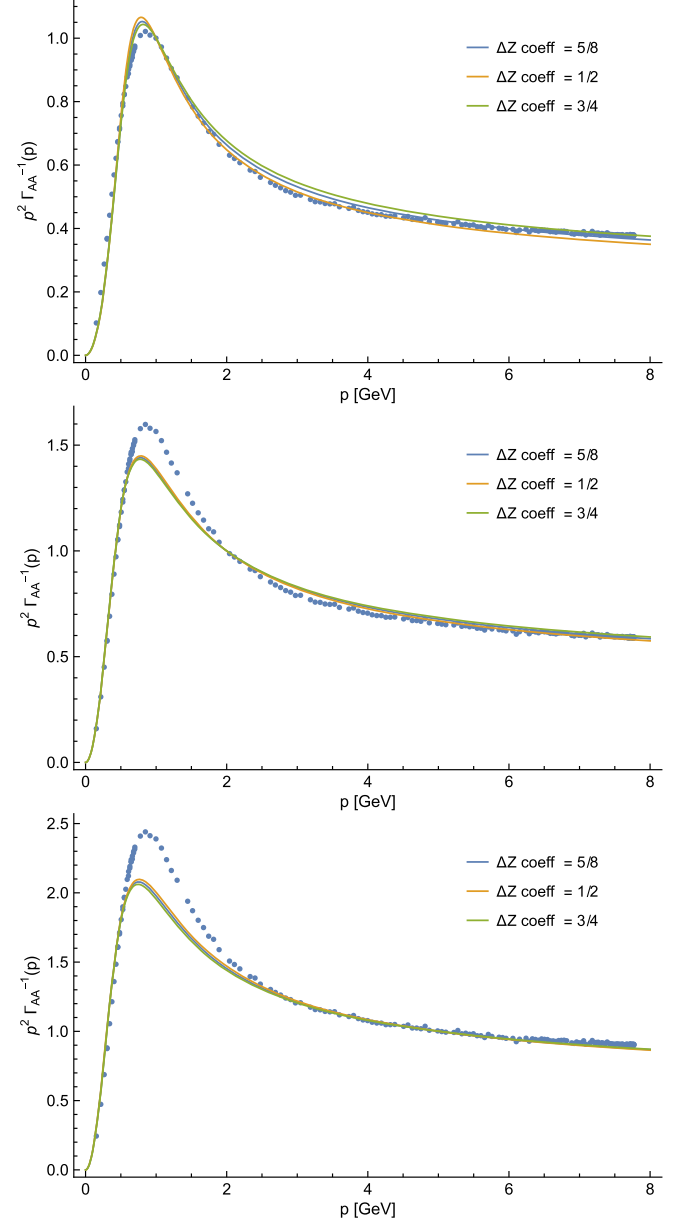


FIG. 6. RG-improved gluon form factor in the DIS scheme at different initial renormalization scales μ_0 and for different ΔZ 's. Top: $\mu_0 = 1$ GeV. Middle: $\mu_0 = 2$ GeV. Bottom: $\mu_0 = 5$ GeV. See the text for details.

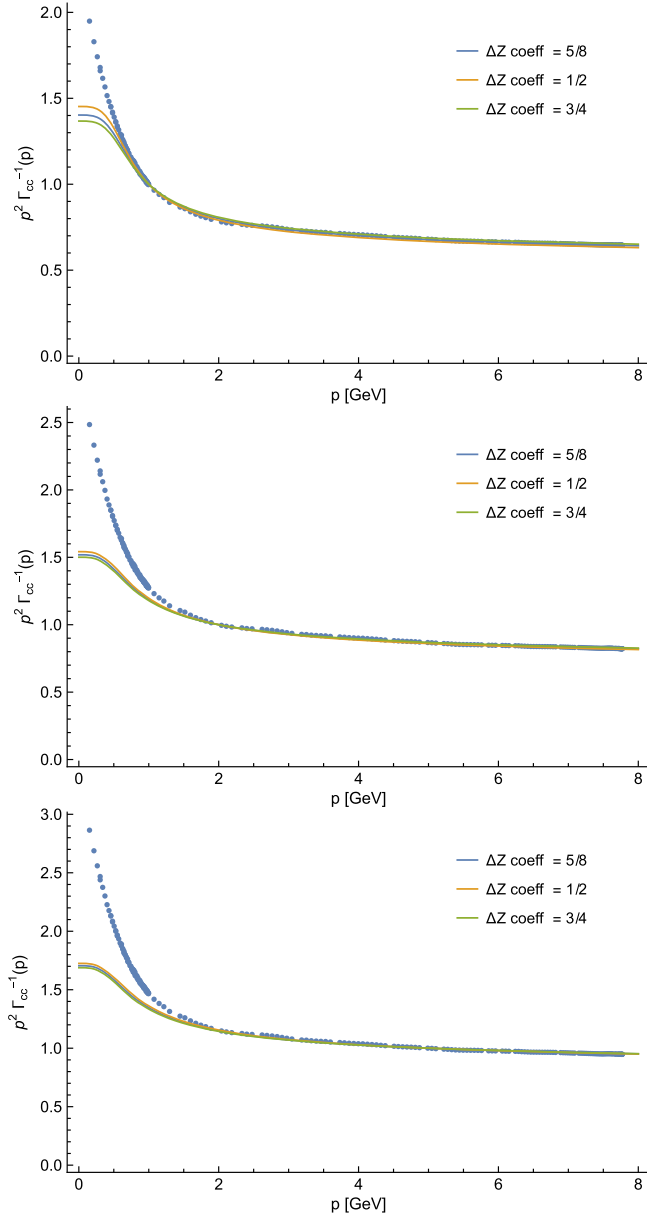


FIG. 7. RG-improved ghost form factor in the DIS scheme at different initial renormalization scales μ_0 and for different ΔZ 's. Plots as in Fig. 6.

It is clear from the fits that increasing or decreasing the value of the coefficient of λ in ΔZ does not have a significant impact on the qualitative behavior of the scheme. Quantitatively, a change in the initial values of the coupling constant λ_0 largely compensates for the difference in the coefficients, although some deviation from our previous results can be observed in the intermediate- to high-energy regime of the gluon sector and in the low-energy regime of the ghost sector at $\mu_0 = 1$ GeV and—less prominently—at $\mu_0 = 2$ GeV.

As for the change of the initial renormalization scale, increasing μ_0 yields a worse match with the lattice data,

TABLE I. Parameters obtained by fitting the lattice data to the DIS scheme RG-improved gluon and ghost form factors, for different initial renormalization scales μ_0 and renormalization parameters ΔZ . The cells contain the values $(\lambda_0, m_0[\text{GeV}])$ of the fitted initial DIS coupling constant $\lambda_0 = \lambda(\mu_0)$ and of the initial DIS gluon mass parameter $m_0 = m_0(\mu_0)$ computed by solving the gap equation.

$\mu_0/\Delta Z$	$\lambda/2$	$5\lambda/8$	$3\lambda/4$
1 GeV	(0.516, 0.673)	(0.473, 0.655)	(0.439, 0.639)
2 GeV	(0.179, 0.622)	(0.168, 0.587)	(0.160, 0.560)
5 GeV	(0.085, 0.567)	(0.082, 0.533)	(0.079, 0.505)

especially at intermediate energies in the gluon sector and at low energies in the ghost sector. Nonetheless, we assess that the agreement between the dynamical model or DIS scheme and the lattice can be still considered satisfactory, given that the present results are obtained by a one-loop calculation and by fitting a single free parameter.

G. SU(2)

To end our overview of the dynamical model, we should mention that some preliminary tests were performed in order to evaluate whether the DIS scheme is also capable of capturing, qualitatively and quantitatively speaking, the SU(2) pure Yang-Mills dynamics. In general, as displayed in Figs. 8 and 9, these tests showed a worse agreement with the lattice data of [34,44–46] in comparison to SU(3). We believe this could be mostly due to a failure of the simple one-loop approximation in the ghost sector, exemplified by the fact that we were not able to obtain a fit of the lattice data for the ghost form factor alone.

In more detail, we performed simple two-parameter fits of the SU(2) gluon and ghost form factors, both separately and simultaneously, at the initial renormalization scale $\mu_0 = 1$ GeV. The simultaneous fit of the two form factors—shown in Fig. 8—yielded an unsatisfactory agreement with the lattice data of [34,44–46], especially in the gluon sector. A good match of the gluon form factor or propagator, on the other hand, was obtained at the expense of the ghost form factor by fitting the former on its own—see Fig. 9. Interestingly, in this second case, the fitted value of the coupling constant $\lambda(\mu_0) = 0.35$ was found to be nearly half that obtained by simultaneously fitting the two form factors—i.e., $\lambda(\mu_0) = 0.59$. As for the fit of the ghost form factor alone, our employed algorithm was not able to reach convergence and provide us with meaningful values of the parameters.

Some insight into these results can be gained by taking the Curci-Ferrari model as a reference. A reiteration of the SU(2) Curci-Ferrari fits [8] using the procedure described in footnote 11—see Figs. 8 and 9—displays most of the features we just reported for the DIS scheme: fitting the gluon form factor alone does not yield a good agreement

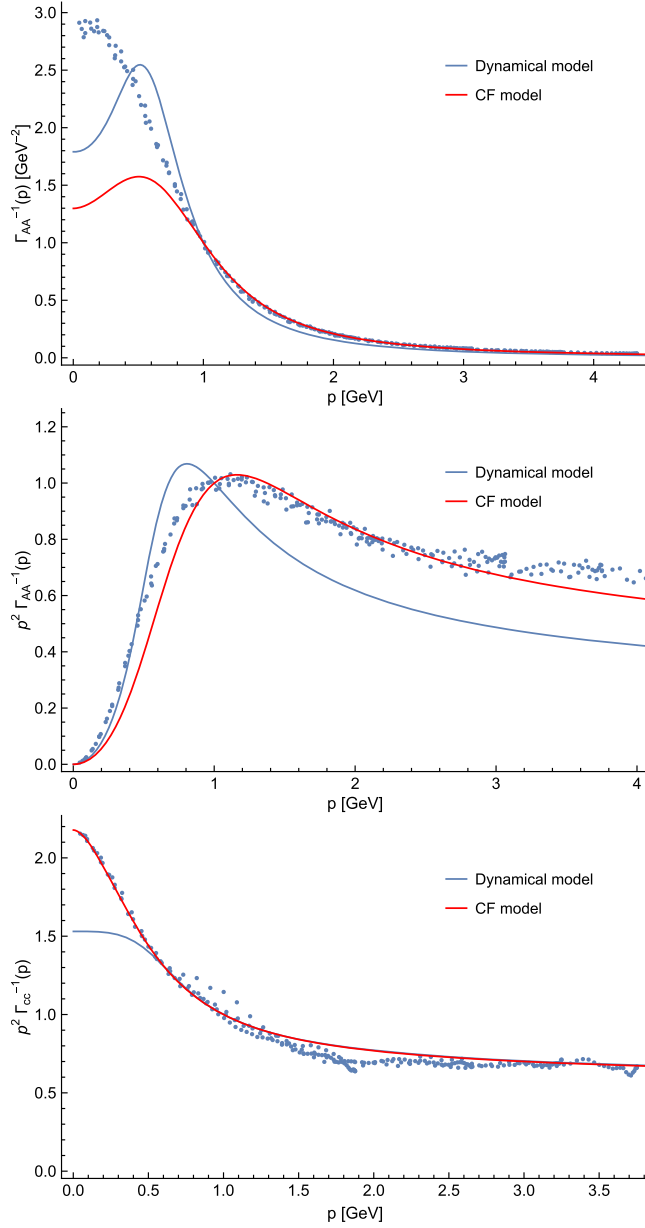


FIG. 8. RG-improved SU(2) gluon propagator (top), gluon form factor (middle) and ghost form factor (bottom) in the DIS scheme, renormalized at $\mu_0 = 1$ GeV, together with the lattice data of [34,44–46] and analogous CF model results (red curves) for comparison. The gluon and the ghost form factors were fitted simultaneously; see the text for details.

with the lattice data for the ghost sector, which only improves when a simultaneous fit of both the form factors is performed; this in turn requires a more-than-doubled value of the coupling constant¹² and leads to a worse match in the gluon sector. We should note that, as far as the dynamical model or DIS scheme is concerned, this kind of

¹² $\lambda(\mu_0) = 0.63$ and $\lambda(\mu_0) = 0.30$ for the simultaneous gluon-ghost and gluon-only CF fits, respectively.

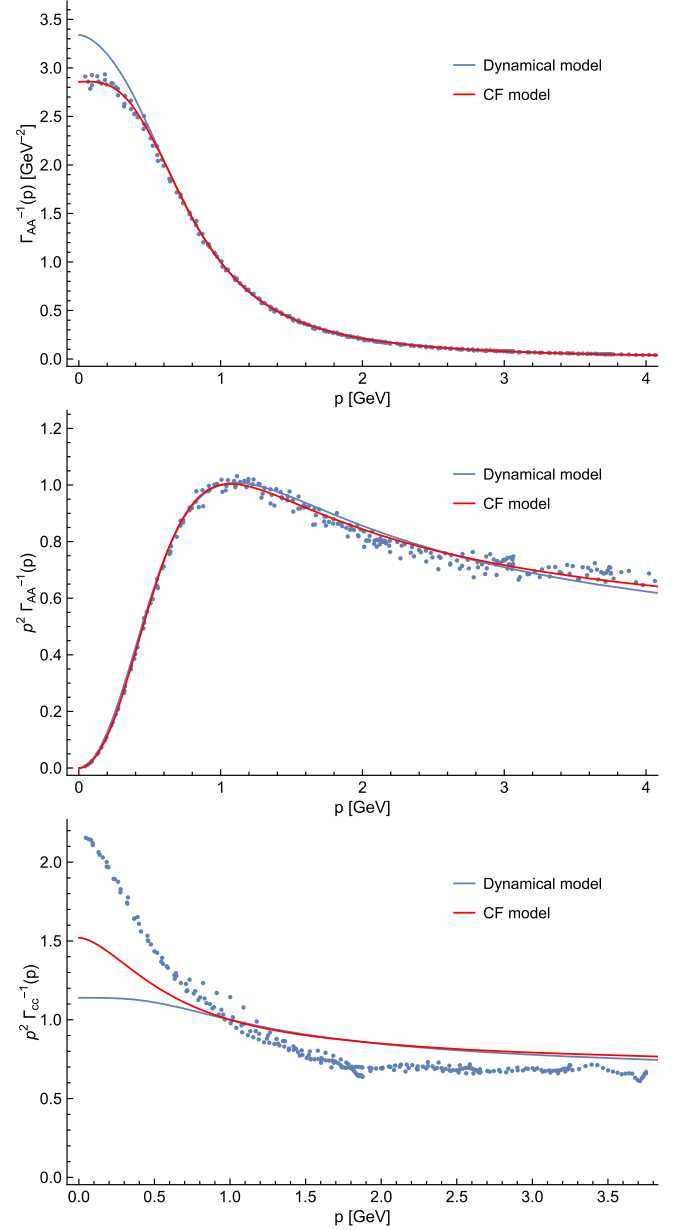


FIG. 9. RG-improved SU(2) gluon propagator (top), gluon form factor (middle) and ghost form factor (bottom) in the DIS scheme, renormalized at $\mu_0 = 1$ GeV, together with the lattice data of [34,44–46] and analogous CF model results (red curves) for comparison. Fit of the gluon form factor alone; see the text for details.

behavior is unseen in SU(3), where fitting the lattice data to the gluon and/or the ghost form factors, either simultaneously or separately, yields essentially the same value of the coupling constant.¹³ Despite these similarities, however, there is one major difference between the two models: just

¹³At $\mu_0 = 1$ GeV, $\lambda(\mu_0) = 0.47$ and $\lambda(\mu_0) = 0.48$ for the one-parameter gluon-only and ghost-only DIS SU(3) fits, respectively.

like in SU(3), instead of quickly saturating and deviating from the lattice data as in the DIS scheme, the one-loop RG-improved Curci-Ferrari ghost form factor manages to reproduce the data well down into the deep IR. In fact, at variance with the DIS scheme, fitting the ghost form factor alone is actually possible within the CF model—at the price of a further increase in the value of the coupling constant.¹⁴

We can then conclude that two main factors are at play in making the DIS scheme perform worse in SU(2) than in SU(3): (i) at one loop, a suboptimal agreement within the ghost sector makes it harder to obtain a good overall fit of the lattice data; (ii) this mismatch pushes toward larger values of the coupling constant, where the one-loop approximation is less trustworthy. Since finding a good two-parameter fit of the SU(2) data was not possible within the present approach, we did not try implementing the gap equation and attempt a one-parameter fit. We leave a more in-depth analysis of the SU(2) case to a future study.

IV. CONCLUSIONS

We showed that the nonvanishing of a nonlocal BRST-invariant mass dimension-two condensate in pure Yang-Mills theory can be probed in any linear covariant gauge by minimizing an effective potential for the condensate, leading to a dynamical gluon mass which value is fixed in terms of a gap equation. For renormalization purposes of the potential, we had to introduce a novel coupling, but by resorting to a procedure known as the reduction of couplings, this parameter could be expressed as a power series in the usual coupling constant.

The computation of the potential and condensate was carried out in Landau gauge, in which case the nonlocal condensate reduces to just $\langle A^2 \rangle$ and computations drastically simplify.

The renormalization group improvement of the gluon and ghost propagators was performed in a newly introduced renormalization scheme termed the dynamically infrared-safe scheme. In the infrared, the dynamically massive model reproduces the expected, nonperturbative behavior of pure Yang-Mills theory not only qualitatively—by the saturation of the gluon propagator at zero momentum—but also quantitatively, as demonstrated by a comparison with the lattice data. In the UV, where the effects of the gluon condensate are negligible as shown explicitly by renormalization group arguments, it reduces to ordinary perturbation theory.

Our results thus indicate that the BRST-invariant gluon condensate is a good candidate for explaining by which mechanism dynamical mass generation occurs in the gluon sector of pure Yang-Mills theory.¹⁵ Albeit that the

eventually dynamically massive model shares many similarities with the Curci-Ferrari model, it is different as highlighted in the text.

A logical next step would be to extend the propagator and renormalization group analysis to other linear covariant gauges, in which case the Nielsen identities [53–56] might prove valuable to get a grip on the gauge (in)dependent contributions. Going beyond the Landau gauge will also require to take into proper account the then explicit non-local nature of the condensate, based on [57].

ACKNOWLEDGMENTS

G. C. acknowledges financial support from the Istituto Nazionale di Fisica Nucleare (INFN), “Strongly Interacting Matter at high density and temperature” (SIM) project, and from the University of Catania, “Linea di Intervento 2 for HQCDyn”. D. D. acknowledges financial support from École Polytechnique (Institut Polytechnique de Paris) and from Centre national de la recherche scientifique (CNRS), next to the warm hospitality at Centre de Physique Théorique (CPhT), which made possible this work. S. P. S. would like to thank the Brazilian agencies Conselho Nacional de Desenvolvimento Científico e Tecnológico (CNPq) and Fundação de Amparo à Pesquisa do Estado do Rio de Janeiro (FAPERJ) for financial support. This study was financed in part by the Coordenação de Aperfeiçoamento de Pessoal de Nível Superior—Brasil (CAPES)—Financial Code 001 (M. N. F.).

APPENDIX A: PERTURBATIVE DECOUPLING OF THE DETERMINANT $\det(\Lambda(\xi))$ IN DIMENSIONAL REGULARIZATION

In order to localize the BRST-invariant gluon field A_μ^h , in Sec. II A we introduced a unity into the partition function in the form

$$1 = \mathcal{N} \int \mathcal{D}\xi \mathcal{D}\tau \mathcal{D}\bar{\eta} \mathcal{D}\eta e^{-S_1} \det(\Lambda(\xi)). \quad (\text{A1})$$

The latter is obtained by a change of variables $F \rightarrow \xi$ in the functional integral

$$\begin{aligned} 1 &= \int \mathcal{D}F \delta(F) = (F = \partial \cdot A^h) \\ &= \int \mathcal{D}\xi \det\left(\frac{\delta(\partial \cdot A^h)}{\delta\xi}\right) \delta(\partial \cdot A^h) \\ &= \int \mathcal{D}\xi \det(-\partial \cdot D(A^h)\Lambda(\xi)) \delta(\partial \cdot A^h), \quad (\text{A2}) \end{aligned}$$

followed by the factorization of the functional determinant and the rewriting of $\det(-\partial \cdot D(A^h))$ in terms of a functional integral over a pair of ghost fields $(\eta, \bar{\eta})$ and of $\delta(\partial \cdot A^h)$ in terms of its τ -Fourier transform. This is analogous to the Faddeev-Popov procedure which is routinely carried out to

¹⁴ $\lambda(\mu_0) = 0.92$ for the ghost-only CF fit.

¹⁵Needless to say, other approaches to dynamical gluon mass generation exist than those mentioned already; see for example [47–52].

derive the partition function of pure Yang-Mills theory in the Landau gauge, with the ghosts η and $\bar{\eta}$ in place of the standard ghost fields c and \bar{c} and the Fourier field τ in place of the Nakanishi-Lautrup field b .

In the context of gauge fixing, thanks to the gauge invariance of the partition function, one usually exchanges A_μ^h for A_μ in (A1) and (A2) by a change of the gluon field integration variables, after which the only ξ -dependent term left in the unity is the determinant $\det(\Lambda(\xi))$. It is easy to see, then, that the ξ -integral decouples from the rest of the partition function, so that the former can be absorbed into the normalization factor \mathcal{N} . On the other hand, our introduction of the unity in Sec. II A is carried out at a stage in which the partition function is already gauge fixed. Therefore, no change of variable $A_\mu^h \rightarrow A_\mu$ can be performed, and, in a generic linear covariant gauge, the nondecoupled field ξ must be treated on the same footing as the other dynamical fields of the theory.

Nevertheless, it can still be shown that the determinant $\det(\Lambda(\xi))$ does not perturbatively contribute to the n -point functions of the theory, as long as it is defined in dimensional regularization. As a consequence, when doing calculations in perturbation theory using dimensional regularization, the determinant can be suppressed by setting $\det(\Lambda(\xi)) = 1$.

In order to prove our statement, we first rewrite the determinant in terms of a functional integral over a new pair of ghost fields $(\lambda, \bar{\lambda})$:

$$\det(\Lambda(\xi)) = \int \mathcal{D}\bar{\lambda}\mathcal{D}\lambda \exp \left\{ - \int d^d x \bar{\lambda}^a \Lambda_{ab}(\xi) \lambda^b \right\}. \quad (\text{A3})$$

Since perturbatively

$$\Lambda_{ab}(\xi) = \delta_{ab} - \frac{g}{2} f_{abc} \xi^c + \frac{g^2}{3!} f_{ace} f_{edb} \xi^c \xi^d + \dots, \quad (\text{A4})$$

we may reexpress (A3) as

$$\det(\Lambda(\xi)) = \int \mathcal{D}\bar{\lambda}\mathcal{D}\lambda e^{-(I_0+I_1)}, \quad (\text{A5})$$

where

$$I_0 = \int d^d x \bar{\eta}^a \eta^a, \quad (\text{A6})$$

$$I_1 = \int d^d x \bar{\eta}^a \Omega_{ab}(\xi) \eta^b, \quad (\text{A7})$$

having defined

$$\Omega_{ab}(\xi) = \Lambda_{ab}(\xi) - \delta_{ab}. \quad (\text{A8})$$

The action term I_1 contains the interaction between $(\lambda, \bar{\lambda})$ and ξ . The latter is quadratic in the ghost fields, with its ξ

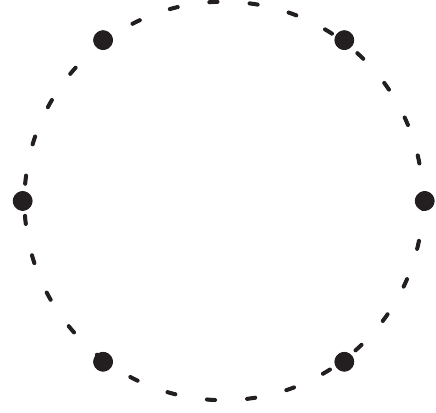


FIG. 10. Loop contributing to the ghost average in (A10) (example for the case $n = 6$). The dashed line is the $(\lambda, \bar{\lambda})$ zero-order propagator.

dependence encoded in the function $\Omega_{ab}(\xi)$. I_0 , on the other hand, contains the zero-order ghost propagator, which is easily seen to be $Q^{ab}(p) = \delta^{ab}$ in momentum space or $Q^{ab}(x) = \delta^{ab} \delta(x)$ in coordinate space.

Now, consider the vacuum expectation value $\langle \mathcal{O} \rangle$ of an operator \mathcal{O} which does not depend on the newly introduced fields $(\lambda, \bar{\lambda})$. This can be computed as

$$\begin{aligned} \langle \mathcal{O} \rangle &= \frac{\langle \mathcal{O} e^{-I_1} \rangle_0}{\langle e^{-I_1} \rangle_0} = \langle \mathcal{O} e^{-I_1} \rangle_{0,\text{conn}} \\ &= \sum_{n=0}^{+\infty} \frac{(-1)^n}{n!} \langle \mathcal{O} I_1^n \rangle_{0,\text{conn}}, \end{aligned} \quad (\text{A9})$$

where the subscript 0 denotes that the average is to be taken with respect to the action I_0 plus any other $(\lambda, \bar{\lambda})$ -independent term originally present in the full action of the theory. $\langle \mathcal{O} I_1^n \rangle_{0,\text{conn}}$ explicitly reads

$$\begin{aligned} \langle \mathcal{O} I_1^n \rangle_{0,\text{conn}} &= \int \prod_{i=1}^n d^d x_i \left\langle \mathcal{O} \prod_{j=1}^n \Omega_{a_j b_j}(\xi(x_j)) \right\rangle_{00,\text{conn}} \\ &\quad \times \langle \bar{\lambda}^{a_1}(x_1) \lambda^{b_1}(x_1) \dots \bar{\lambda}^{a_n}(x_n) \lambda^{b_n}(x_n) \rangle_{\text{gh},\text{conn}}, \end{aligned} \quad (\text{A10})$$

where the subscript 00 denotes that the first average is to be taken with respect to the full, $(\lambda, \bar{\lambda})$ -independent action, whereas the subscript “gh” denotes that the second average is to be taken with respect to the zero-order ghost action I_0 . Diagrammatically, for each $n \geq 1$, the ghost average receives contributions from a single ghost loop, depicted in Fig. 10. In coordinate space, suppressing the color structure, the diagram reads

$$(-1)(n-1)! \delta(x_1 - x_2) \dots \delta(x_{n-1} - x_n) \delta(x_n - x_1) \quad (\text{A11})$$

or, equivalently,

$$(-1)(n-1)!\delta(0) \int d^d x \prod_{i=1}^n \delta(x_i - x), \quad (\text{A12})$$

where $\delta(0)$ is a Dirac delta in coordinate space:

$$\delta(0) = \int \frac{d^d q}{(2\pi)^d} 1. \quad (\text{A13})$$

Therefore, for $n \geq 1$,

$$\begin{aligned} \langle \mathcal{O}I_1^n \rangle_{0,\text{conn}} &= (-1)(n-1)!\delta(0) \\ &\times \int d^d x \langle \text{CTr}\{\Omega^n(\xi(x))\} \rangle_{00,\text{conn}}, \end{aligned} \quad (\text{A14})$$

where $\Omega^n(\xi)$ is the matrix product of n factors of $\Omega(\xi)$ and the trace is taken over the color indices.

In dimensional regularization, the integral in (A13) vanishes [58]. It follows that $\langle \mathcal{O}I_1^n \rangle_{0,\text{conn}} = 0$ for every $n \geq 1$, so that, going back to (A9),

$$\langle \mathcal{O} \rangle = \langle \mathcal{O} \rangle_0 = \langle \mathcal{O} \rangle_{00}, \quad (\text{A15})$$

where to obtain $\langle \mathcal{O} \rangle_{00}$ we have integrated out the free ghost action I_0 from $\langle \mathcal{O} \rangle_0$. What (A15) means is that the perturbative corrections to the vacuum expectation value $\langle \mathcal{O} \rangle$ due to the determinant $\det(\Lambda(\xi))$ vanish in dimensional regularization. Therefore, the vacuum expectation value of any operator \mathcal{O} in the full theory can be computed by setting $\det(\Lambda(\xi)) = 1$ in its dimensionally regularized partition function.

One may have noticed that our proof—aside from dimensional regularization—relies exclusively on the fact that $\Lambda(\xi)$ is equal to the unit matrix to lowest order in perturbation theory. The question arises, then, whether the proof is general enough to apply to the determinant of any such matrix. The answer is that, in general, it does not. Indeed, setting $\delta(0) = 0$ in dimensional regularization is allowed if and only if the calculations can be carried out without spoiling the symmetries of the theory.

While Lorentz invariance is clearly preserved by the action in (A3), showing that the latter does not violate the BRST invariance of the full action of the theory requires us to extend the symmetry to the ghost fields λ and $\bar{\lambda}$. Indeed, a straightforward calculation starting from (11) and the definition of $\Lambda_{ab}(\xi)$ in (3) yields

$$s\Lambda_{ab}(\xi) = \Lambda_{ac}(\xi)\Psi_b^c(c, \xi), \quad (\text{A16})$$

with

$$\Psi_b^a(c, \xi) = -\frac{\partial(s\xi^a)}{\partial\xi^b}, \quad (\text{A17})$$

so that the ghosts must have nonvanishing BRST transformations if (A3) is to be invariant. Since the BRST

transformation does not act on the antighost index of $\Lambda_{ab}(\xi)$, it is reasonable to define

$$s\lambda^a = -\Psi_b^a(c, \xi)\lambda^b, \quad s\bar{\lambda}^a = 0, \quad (\text{A18})$$

where $s\lambda^a$ is chosen so that $s(\Lambda\lambda) = 0$. (A3)—and the full action of the theory together with it—is invariant with respect to these extended BRST transformations. The nilpotency of the extended BRST operator is then easily proved by observing that $s^2\Lambda_{ab}(\xi) = 0$ —which holds thanks to the nilpotency of s on the fields ξ and c —implies that

$$0 = s^2\Lambda_{ab} = \Lambda_{ac}(\Psi_d^c\Psi_b^d + s\Psi_b^c), \quad (\text{A19})$$

that is, $s\Psi = -\Psi^2$. When plugged into (A18), the latter ensures that $s^2\lambda^a = s^2\bar{\lambda}^a = 0$.

APPENDIX B: UNITY AT WORK

As shown in the main text, a one-loop computation shows that the σ action with $\sigma \rightarrow \sigma_0 + \delta\sigma$ leads to

$$\Pi^{1\text{-loop}} = p^2 + m^2 + \Pi_{\text{CF}}^{1\text{-loop}}(p^2, m^2) + \Pi_{\text{extra}}^{1\text{-loop}} \quad (\text{B1})$$

where the mass term will be canceled by the self-energy contributions originating from the extra terms in the action, when using the gap equation $\frac{\partial V}{\partial\sigma} = 0$ [cf. (43)]. With the “extra” part, we mean the diagrams that are generated by the extra vertices arising from the $\delta\sigma$ part of the σ Lagrangian, meaning the $\delta\sigma A^2$ and A^4 vertices; see Eqs. (31) and (32).

This will actually be a more generic feature of the dynamical model. More precisely, the tree-level mass will always cancel against certain contributions coming from the extra diagrams.

Let us now try to show this by making use of the “power of unity.” We will work with a simplified notation, to make things clear. But the general argument readily applies to the case under study.

Let us consider a theory, Theory 1, with a partition function $\int[dA]e^{-S(A)}$, but we could also add a unity to get Theory 2 with a partition function

$$\int \mathcal{D}A e^{-\frac{1}{\hbar}S(A)} \times \int \mathcal{D}\sigma e^{-\frac{1}{\hbar} \int d^d x \left(\sigma - \frac{gA^2}{2}\right)^2}. \quad (\text{B2})$$

We understand that this is still the same theory as the (exact) Gaussian integral over σ yields a unity.¹⁶ This means that (connected) correlation functions remain unchanged: $\langle A\dots A \rangle_1 = \langle A\dots A \rangle_2$.¹⁷ We have temporarily introduced the (loop counting) factor \hbar . Clearly, by identifying order per order in \hbar , the equivalence between

¹⁶We did not write global normalization factors.

¹⁷With “A” a shorthand for all original fields.

$\langle A\dots A \rangle_1$ and $\langle A\dots A \rangle_2$ will also hold order per order in perturbation theory, seen as formal power series in \hbar .

Let us illustrate it explicitly: the extra vertices introduced by the unity, (31) and (32), are visually represented by



We get at one-loop a contribution proportional to

$$\langle AA \rangle_{extra}^{comm} = \text{diagram 1} + \text{diagram 2} + \text{diagram 3} = 0. \quad (\text{B3})$$

Using the trivial (constant) propagator $\langle \sigma \sigma \rangle = 1$ and the correct symmetry factors, we end up with

$$\langle AA \rangle_{extra}^{1PI} = g^2 \int \langle AA \rangle + \frac{1}{2} g^2 \int \langle AA \rangle - \frac{3}{2} g^2 \int \langle AA \rangle, \quad (\text{B4})$$

which is indeed equal to zero.

Next, we consider the possibility that σ develops a vacuum expectation value, namely

$$\sigma \rightarrow \langle \sigma \rangle + \delta\sigma \equiv \sigma + \delta\sigma \quad (\text{B5})$$

with per definition $\langle \delta\sigma \rangle = 0$. In this case, the partition function will read

$$\int \mathcal{D}A e^{-S[A] - \int d^4x g\sigma A^2} \int \mathcal{D}\delta\sigma e^{-\frac{1}{2} \int d^4x (\delta\sigma - \frac{gA^2}{2})^2} e^{-\int d^4x (\frac{\sigma}{2})}. \quad (\text{B6})$$

The first exponential will still yield a unity; the second consists of a constant and will play no role in correlation functions (but it does in the quantum effective action). The term linear in $\delta\sigma$ we dropped, as this will cancel order per order by removing all $\delta\sigma$ -tadpole graphs, which is equivalent to $\langle \delta\sigma \rangle \equiv 0$, or, extremization of the effective action with respect to σ , that is, the gap equation; see e.g. [28]. Finally, there is also an effective mass term for the A field that we included in the original action, that is, with a “dynamically massive” A field.

At one loop, we would now get

$$\langle AA \rangle_{extra}^{comm} = \text{diagram 1} + \text{diagram 2} + \text{diagram 3} = \text{diagram 4} + \text{diagram 5}. \quad (\text{B7})$$

These two diagrams are completely similar to those in the last line of (40); when resummed into the inverse propagator they will annihilate the tree-level mass term upon using the gap equation $\frac{\partial V}{\partial \sigma} = 0$, as it follows from direct computation also here. The first diagram in the first line is nonzero, but it will cancel against other (nonwritten) tadpole contributions. Notice that we did not explicitly use the underlying unity at this point.

We can reconsider the three diagrams in the first line of (B7) also from the unity viewpoint though. In that case, the three diagrams cancel against each other, just as before. However, this means we have removed one, but not all, tadpole contributions, meaning that there will be a net tadpole correction to $\langle AA \rangle_{extra}^{1PI}$, which actually corresponds to minus the first diagram, upon amputating the external A legs of course. But due to the gap equation, this is nothing else than the tree-level mass, up to the sign.

It is clear this observation will continue to hold through at any order n : we can always keep the necessary tadpole (sub)graphs to get all diagrams that make up the unity order per order (the sum of which diagrams will then lead to a zero), and the remaining contribution will be the (usually never written) “counterterm” that eliminates the tadpoles, up to the sign. As at one loop, this will exactly kill the tree-level mass due to the gap equation. Overall, we will thus be left by the same diagrams of the Curci-Ferrari model, up to the tree-level mass. Notice though that the mass running in the loops will still need an appropriate reexpansion up to the considered order, as the actual mass is defined from $m^2 \equiv -\mu^\epsilon \sigma / \zeta(g^2)$; see Eq. (25). This will lead to further differences with the Curci-Ferrari case.

APPENDIX C: A FEW MORE WORDS ABOUT THE EFFECTIVE POTENTIAL

In (81), we constructed an RG improved potential up to leading log (LL) order. The solution (86) corresponds to a genuine stationary point as $\frac{\partial V_{LL}}{\partial m} = 0$. Upon closer inspection we notice it actually corresponds to a minimum of

$\text{Re}(V)$ and a maximum of $\text{Im}(V)$. We kept however using (86) as a solution to the gap equation in the remainder of the paper.¹⁸ Before discussing the validity of this approximation, we note that we chose to minimize $V_{LL}(m(\bar{\mu}))$ with respect to the variable $m(\bar{\mu})$. Up to the considered order, as noted below (85), one can reinterpret it in terms of $V(m(\bar{\mu} = m))$ and thence minimize with respect to $m(m)$ rather than $m(\bar{\mu})$. We did not do so, as our eventual interest lies in the RG flow of the propagators in the DIS scheme, with initial conditions set at $\bar{\mu}_0$. This would require, after having minimized with respect to $m(m)$, to flow this $\overline{\text{MS}}$ solution from $\bar{\mu} = m$ to $\bar{\mu} = \bar{\mu}_0$ using the $\overline{\text{MS}}$ anomalous dimensions, followed by converting it to the desired initial value in the DIS scheme via the conversion (87). As we do not expect the $\overline{\text{MS}}$ scheme to be trustworthy at lower scales, we intentionally first set $\bar{\mu} = \bar{\mu}_0$ and then directly extract an estimate for the $\overline{\text{MS}}$ initial conditions at the chosen, high enough, scale $\bar{\mu}_0$, followed by the conversion to DIS.

In passing, we notice here that for the LL minimum solution (86), $\bar{\mu} \frac{d}{d\bar{\mu}} m_{\text{sol},\overline{\text{MS}}} = 0$ up to the considered order. Although it might look strange to find a RG-invariant solution of the LL gap equation, this will be always the case in the LL case, which after all is based on the zeroth-order (“classical”) potential, dressed with logs. This common feature can be easily checked using the related formalisms of [40,41] as for single scale theory, the LL potential will always have the structure of (85) with a solution similar to (86). This no running of the solution is thus an artifact of the LL approximation.

This being said, we can now have a look at what happens when we include the next-to-leading-log (NLL) corrections. As we know the first term of the NLL series, we can use this to our advantage. Indeed, generalizing (81), we may write

$$\begin{aligned} V_{\text{NLL}}(m) &= \frac{9}{13} \frac{N^2 - 1}{N} \frac{m^4}{2g^2} \left(\sum_{n=0}^{\infty} v_n u^n + g^2 \sum_{n=0}^{\infty} w_n u^n \right) \\ &= \frac{9}{13} \frac{N^2 - 1}{N} \frac{m^4}{2g^2} (F(u) + g^2 G(u)), \end{aligned} \quad (\text{C1})$$

where $w_0 = -\frac{113N}{288\pi^2}$, as it follows from (29). The function $F(u)$ was already determined in (84), and upon imposing (80) to next-to-leading order, we get

$$\begin{aligned} &(\beta_1 + \gamma_1)F(u) + \gamma_0 G(u) \\ &- (1 + \beta_0 u)G'(u) + \left(\frac{\gamma_0}{2} - \beta_1 u \right) F'(u) = 0, \end{aligned} \quad (\text{C2})$$

¹⁸There is actually also the solution at $m^2 = 0$. However, this is not to be trusted. To keep the expansion under control, we should then assume $\mu \sim 0$, implying $g^2 \sim \infty$ in the $\overline{\text{MS}}$ scheme, thence invalidating the expansion. The relevant expansion parameter at $\bar{\mu}_0 = 1$ GeV, $\lambda_{\overline{\text{MS}}}(\mu_0) = 0.316$, is sufficiently small to trust the used expansion more or less, with moreover $m_{\text{sol}}/\bar{\mu}_0$ close to 1.

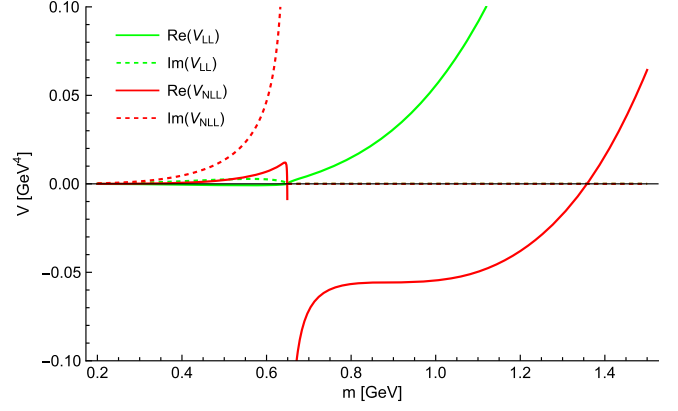


FIG. 11. Leading $V_{LL}(m)$ and next-to-leading log $V_{NLL}(m)$ renormalization group improved effective potential at $\bar{\mu}_0 = 1$ GeV with choice of parameter $\lambda_{\overline{\text{MS}}}(\mu_0) = 0.316$ (see Sec. III E).

which solves uniquely to

$$\begin{aligned} G(u) &= \frac{1}{288\beta_0^2\pi^2} (1 + \beta_0 u)^{\gamma_0/\beta_0} (-113N\beta_0^2 - 288\beta_0\beta_1\gamma_0\pi^2 u \\ &+ 288\beta_0\gamma_1\pi^2 u + \ln(1 + \beta_0 u)\pi^2(288\beta_0\beta_1 \\ &+ 144\beta_0^2\gamma_0 + 288\beta_1\gamma_0 + 288\beta_1\gamma_0^2 + 144\beta_0\gamma_0^2)). \end{aligned} \quad (\text{C3})$$

As a check on this result, reexpanding (C1) up to order g^2 gives the correct terms upon comparison with the two-loop $\overline{\text{MS}}$ effective potential as it was computed first in [18], later on verified in [59], up to the constant term of the two-loop piece of course, which is the first of the next-to-next-to-leading log order terms.

Focusing on the SU(3) case and setting as before $\lambda_{\overline{\text{MS}}}(\mu_0) = 0.316$ at $\bar{\mu} = \mu_0 = 1$ GeV, we come to Fig. 11, where both the LL and NLL potential are shown. We see that going to next-to-leading log order in the RG improved expansion does shift the location of the minimum to around 0.8 GeV, but it does land in the region where the improved NLL potential is real valued. For the record, we refrain from using this minimum in Sec. III V, as we only solved the two-point functions RG flow at leading order. Actually, the potential is rather flat in the region of interest, so let us see what happens in terms of a variable $\bar{\mu}$, which will also allow to verify if the expected UV RG asymptotics is reached. We first convert the fit value $\lambda_{\overline{\text{MS}}}(\mu_0) = 0.316$ into the corresponding $\Lambda_{\overline{\text{MS}}}$ value through inversion of the two-loop expression

$$g^2(\bar{\mu}) = \frac{1}{\beta_0 \ln \frac{\bar{\mu}^2}{\Lambda_{\overline{\text{MS}}}^2}} \left(1 - \frac{\beta_1}{\beta_0 \beta_0} \frac{\ln \ln \frac{\bar{\mu}^2}{\Lambda_{\overline{\text{MS}}}^2}}{\ln \frac{\bar{\mu}^2}{\Lambda_{\overline{\text{MS}}}^2}} \right) \quad (\text{C4})$$

at $\bar{\mu} = \mu_0$, yielding $\Lambda_{\overline{\text{MS}}} = 0.630$ GeV. Feeding this and (C4) back into $V_{\text{NLL}}(m)$ allows one to show the potential

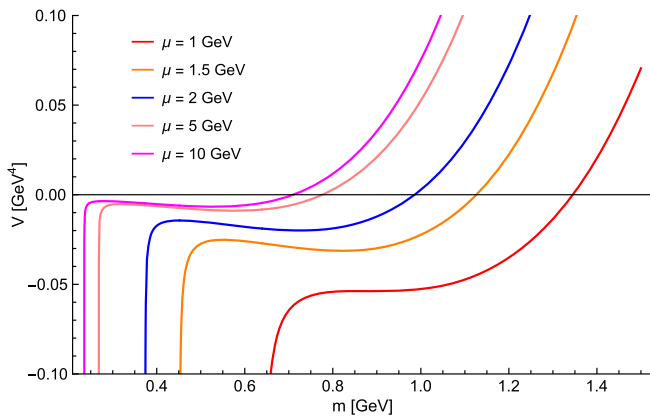


FIG. 12. Next-to-leading log $V_{\text{NLL}}(m)$ renormalization group improved effective potential for various values of $\bar{\mu}$.

for various values of $\bar{\mu}$, as shown in Fig. 12. We observe a clear, real-valued minimum which lowers for growing $\bar{\mu}$. At last, solving for the minimum leads to Fig. 13, shown together with a fitted (over the interval $\mu = [5, 10]$ GeV)

$$M(\bar{\mu}) = 0.571 \left(\ln \frac{\bar{\mu}}{\Lambda_{\overline{\text{MS}}}} \right)^{-9/88}, \quad (\text{C5})$$

consistent with the expected UV RG behavior in terms of $\partial \ln m / \partial \ln \bar{\mu} = (\gamma_0/2)g^2 + \dots$. For too low values of $\bar{\mu}$, i.e., too close to the $\overline{\text{MS}}$ Landau pole at $\bar{\mu} = \Lambda_{\overline{\text{MS}}}$, we should not trust the results anymore. The Landau pole is eventually also what pushes the potentials in Fig. 12 to $-\infty$

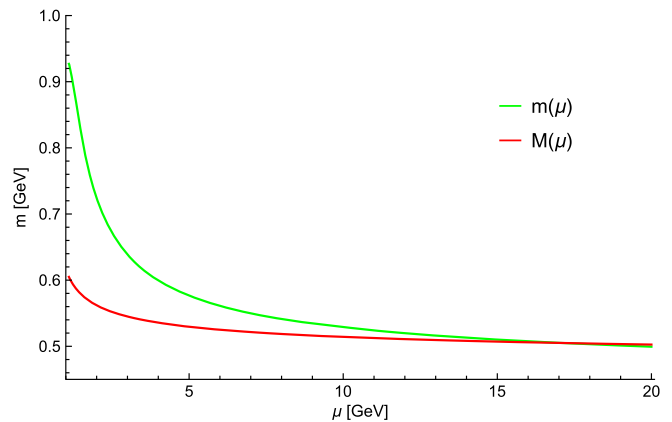


FIG. 13. Running minimum of $V_{\text{NLL}}(m)$ (green) compared to the expected UV asymptotics (red); see Eq. (C5).

and eventually into the complex region for too small m , making the quantity $\beta_0 g^2(\bar{\mu}) \ln \frac{m^2}{\bar{\mu}^2}$ too large. In any case, log RG resummations capture information from all orders, while the gap equation imposes a further constraint between terms of different orders. It would be interesting to investigate more sophisticated RG improvements of the effective potential, so that for example the RG flow of the solution is strictly consistent with the anomalous dimension of the mass at the chosen order, for any value of the RG scale, but this falls beyond the scope of the current paper. This might also further complicate the numerics (stability) of the fitting procedure. We plan to come back to this in future work.

-
- [1] G. Curci and R. Ferrari, *Nuovo Cimento A* **32**, 151 (1976).
- [2] G. Curci and R. Ferrari, *Nuovo Cimento A* **35**, 1 (1976); **47**, 555(E) (1978).
- [3] J. A. Gracey, *Phys. Lett. B* **552**, 101 (2003).
- [4] M. Tissier and N. Wschebor, *Phys. Rev. D* **82**, 101701 (2010).
- [5] M. Tissier and N. Wschebor, *Phys. Rev. D* **84**, 045018 (2011).
- [6] M. Peláez, M. Tissier, and N. Wschebor, *Phys. Rev. D* **88**, 125003 (2013).
- [7] U. Reinosa, J. Serreau, M. Tissier, and N. Wschebor, *Phys. Rev. D* **96**, 014005 (2017).
- [8] J. A. Gracey, M. Peláez, U. Reinosa, and M. Tissier, *Phys. Rev. D* **100**, 034023 (2019).
- [9] P. Dall’Olio and A. Weber, *Ann. Phys. (Amsterdam)* **439**, 168801 (2022).
- [10] M. Peláez, U. Reinosa, J. Serreau, M. Tissier, and N. Wschebor, *Rep. Prog. Phys.* **84**, 124202 (2021).
- [11] N. Barrios, J. A. Gracey, M. P. and, and U. Reinosa, *Phys. Rev. D* **104**, 094019 (2021).
- [12] U. Reinosa, J. Serreau, M. Tissier, and N. Wschebor, *Phys. Rev. D* **91**, 045035 (2015).
- [13] U. Reinosa, J. Serreau, M. Tissier, and A. Tresmontant, *Phys. Rev. D* **95**, 045014 (2017).
- [14] J. Maelger, U. Reinosa, and J. Serreau, *Phys. Rev. D* **98**, 094020 (2018).
- [15] J. Serreau and M. Tissier, *Phys. Lett. B* **712**, 97 (2012).
- [16] M. Tissier, *Phys. Lett. B* **784**, 146 (2018).
- [17] U. Reinosa, J. Serreau, R. C. Terin, and M. Tissier, *SciPost Phys.* **10**, 035 (2021).
- [18] H. Verschelde, K. Knecht, K. Van Acoleyen, and M. Vanderkelen, *Phys. Lett. B* **516**, 307 (2001).
- [19] W. Zimmermann, *Commun. Math. Phys.* **97**, 211 (1985).
- [20] S. Heinemeyer, M. Mondragón, N. Tracas, and G. Zoupanos, *Phys. Rep.* **814**, 1 (2019).
- [21] G. Dell’Antonio and D. Zwanziger, *Commun. Math. Phys.* **138**, 291 (1991).
- [22] M. Lavelle and D. McMullan, *Phys. Rep.* **279**, 1 (1997).
- [23] M. A. L. Capri, D. Dudal, D. Fiorentini, M. S. Guimaraes, I. F. Justo, A. D. Pereira, B. W. Mintz, L. F. Palhares, R. F. Sobreiro, and S. P. Sorella, *Phys. Rev. D* **92**, 045039 (2015).

- [24] H. Verschelde, *Phys. Lett. B* **351**, 242 (1995).
- [25] K. Knecht and H. Verschelde, *Phys. Rev. D* **64**, 085006 (2001).
- [26] D. Dudal, H. Verschelde, and S. P. Sorella, *Phys. Lett. B* **555**, 126 (2003).
- [27] R. Jackiw, *Phys. Rev. D* **9**, 1686 (1974).
- [28] M. E. Peskin and D. V. Schroeder, *An Introduction to Quantum Field Theory* (Addison-Wesley, Reading, 1995).
- [29] M. A. L. Capri, D. Dudal, M. S. Guimaraes, A. D. Pereira, B. W. Mintz, L. F. Palhares, and S. P. Sorella, *Phys. Lett. B* **781**, 48 (2018).
- [30] H. Verschelde, S. Schelstraete, and M. Vanderkelen, *Z. Phys. C* **76**, 161 (1997).
- [31] R. E. Browne, D. Dudal, J. A. Gracey, V. E. R. Lemes, M. S. Sarandy, R. F. Sobreiro, S. P. Sorella, and H. Verschelde, *J. Phys. A* **39**, 7889 (2006).
- [32] V. N. Gribov, *Nucl. Phys.* **B139**, 1 (1978).
- [33] D. Kroff and U. Reinosa, *Phys. Rev. D* **98**, 034029 (2018).
- [34] A. Cucchieri, D. Dudal, T. Mendes, and N. Vandersickel, *Phys. Rev. D* **93**, 094513 (2016).
- [35] F. Siringo, *Phys. Rev. D* **92**, 074034 (2015).
- [36] F. Siringo and G. Comitini, *Phys. Rev. D* **98**, 034023 (2018).
- [37] G. Comitini and F. Siringo, *Phys. Rev. D* **102**, 094002 (2020).
- [38] A. G. Duarte, O. Oliveira, and P. J. Silva, *Phys. Rev. D* **94**, 014502 (2016).
- [39] D. Dudal, R. F. Sobreiro, S. P. Sorella, and H. Verschelde, *Phys. Rev. D* **72**, 014016 (2005).
- [40] B. M. Kastening, *Phys. Lett. B* **283**, 287 (1992).
- [41] M. Bando, T. Kugo, N. Maekawa, and H. Nakano, *Phys. Lett. B* **301**, 83 (1993).
- [42] D. Dudal, O. Oliveira, and P. J. Silva, *Ann. Phys. (Amsterdam)* **397**, 351 (2018).
- [43] G. Comitini and F. Siringo, *Phys. Rev. D* **102**, 094002 (2020).
- [44] A. Cucchieri and T. Mendes, *Phys. Rev. Lett.* **100**, 241601 (2008).
- [45] A. Cucchieri and T. Mendes, *Phys. Rev. D* **78**, 094503 (2008).
- [46] A. Cucchieri, D. Dudal, and N. Vandersickel, *Phys. Rev. D* **85**, 085025 (2012).
- [47] A. C. Aguilar and A. A. Natale, *J. High Energy Phys.* **08** (2004) 057.
- [48] A. C. Aguilar, D. Binosi, and J. Papavassiliou, *Phys. Rev. D* **78**, 025010 (2008).
- [49] C. S. Fischer, A. Maas, and J. M. Pawłowski, *Ann. Phys. (Amsterdam)* **324**, 2408 (2009).
- [50] A. K. Cyrol, L. Fister, M. Mitter, J. M. Pawłowski, and N. Strodthoff, *Phys. Rev. D* **94**, 054005 (2016).
- [51] M. Q. Huber, *Phys. Rep.* **879**, 1 (2020).
- [52] J. Horak, F. Ihssen, J. Papavassiliou, J. M. Pawłowski, A. Weber, and C. Wetterich, *SciPost Phys.* **13**, 042 (2022).
- [53] N. K. Nielsen, *Nucl. Phys.* **B101**, 173 (1975).
- [54] M. A. L. Capri, D. Dudal, A. D. Pereira, D. Fiorentini, M. S. Guimaraes, B. W. Mintz, L. F. Palhares, and S. P. Sorella, *Phys. Rev. D* **95**, 045011 (2017).
- [55] M. Napetschnig, R. Alkofer, M. Q. Huber, and J. M. Pawłowski, *Phys. Rev. D* **104**, 054003 (2021).
- [56] F. Siringo and G. Comitini, *Phys. Rev. D* **106**, 076014 (2022).
- [57] M. A. L. Capri, D. M. van Egmond, G. Peruzzo, M. S. Guimaraes, O. Holanda, S. P. Sorella, R. C. Terin, and H. C. Toledo, *Ann. Phys. (Amsterdam)* **390**, 214 (2018).
- [58] J. C. Collins, *Renormalization: An Introduction to Renormalization, The Renormalization Group, and the Operator Product Expansion*, Cambridge Monographs on Mathematical Physics (Cambridge University Press, Cambridge, England, 1986), Vol. 26.
- [59] J. A. Gracey, *Eur. Phys. J. C* **39**, 61 (2005).